Fatma MANCUSUNLUOĞLU

M.S. Thesis in Physics

July - 2011

SPIN POLARIZED TRANSPORT PROPERTIES OF IMPURITY INDUCED CARBON WIRES

by

Fatma MANCUSUNLUOĞLU

July 2011

SPIN POLARIZED TRANSPORT PROPERTIES OF IMPURITY INDUCED CARBON WIRES

by

Fatma Mancusunluoğlu

A thesis submitted to

The Graduate Institute of Sciences and Engineering

of

Fatih University

in partial fulfillment of the requirements for the degree of

Master of Science

in

Physics

July 2011
Istanbul, Turkey

APPROVAL PAGE

I certify that this thesis satisfies all the requirements as a thesis for the degree of Master of Science.

Prof. Dr. Mustafa KUMRU
Head of Department

This is to certify that I have read this thesis and that in my opinion it is fully adequate, in scope and quality, as a thesis for the degree of Master of Science.

Assoc. Prof. Serkan ÇALIŞKAN
Supervisor

Examining Committee Members

Assoc. Prof. Serkan ÇALIŞKAN _____

Assoc. Prof. Bayram ÜNAL _____

Assoc. Prof. Ahmet ALTUN _____

It is approved that this thesis has been written in compliance with the formatting rules laid down by the Graduate Institute of Sciences and Engineering.

Assoc. Prof. Nurullah ARSLAN
Director

July 2011

SPIN POLARIZED TRANSPORT PROPERTIES OF IMPURITY CARBON WIRES

Fatma MANCUSUNLUOĞLU

M.S. Thesis – Physics
July 2011

Supervisor: Assoc. Prof. Serkan ÇALIŞKAN

ABSTRACT

We study spin polarized transport on structures consisting of Carbon wires which may include substitutional impurities. We perform first principle calculations on these structures using the Non equilibrium Green's Function Formalism combined with the Density Functional Theory. The constructed structures, modeled as Small World Networks, through a probability, are found to depend strongly on the geometrical disorder. Spin polarized transport properties of these structures are discussed, by means of numerical results concerning the spin dependent conductance, transmission spectra, density of states and current-voltage characteristics.

Keywords: Spin Polarized Transport, Spintronics, Small World Networks, Density Functional Theory, Non Equilibrium Green's Functional Formalism

KATKILI KARBON TELLERİN SPİNE BAĞLI İLETİM ÖZELLİKLERİ

Fatma MANCUSUNLUOĞLU

Yüksek Lisans Tezi – Fizik
Temmuz 2011

Tez Danışmanı: Doç. Dr. Serkan ÇALIŞKAN

ÖZ

Katkılı Karbon tellerden oluşan yapılarda spin polarize iletimi çalıştık. “Density Functional Theory” ile birlikte “Non Equilibrium Green’s Function” formalizmi kullanılarak bu yapılar üzerine “first principle” hesaplamalarını gerçekleştirdik. “Small World Networks” ile modellenerek, belirli bir olasılıkla, oluşturulan yapıların önemli ölçüde geometriksel düzensizliğe bağlı olduğu bulunmuştur. Spine bağlı iletkenlik, transmisyon spektrumu, durum yoğunluğu ve akım-voltaj karakteristiklerine ilişkin nümerik sonuçlar kullanılarak, bu yapıların spin polarize iletim özellikleri tartışılmıştır.

Anahtar Kelimeler: Spin Polarize Transport, Spintronik, Small World Networks, Density Functional Theory, Non Equilibrium Green’s Function Formalizmi

To Eyüp OĞUZ and my sister Tuba and my parents

ACKNOWLEDGEMENT

First of all, I would like to gratitude to my supervisor Assoc. Prof. Dr. Serkan ÇALIŞKAN for his help, motivation, stimulating and incentive suggestions during whole time of research and for writing this thesis.

I appreciate my colleague, Mrs. Hülya AYTAN for his valuable contributions during all stages of the work.

I express my thanks and appreciation of Eyüp Oğuz and my family for their understanding, motivation, supporting and patience.

Finally, I am thankful to all my friends and colleagues motivating and encouraging me to accomplish the study on time.

TABLE OF CONTENTS

LIST OF FIGURES

FIGURE

LIST OF SYMBOLS AND ABBREVIATIONS

SYMBOL/ABBREVIATION

ATK	: Atomistix Toolkit
CR	: Central Region
$D(E)$	: Density of States
DFT	: Density Functional Theory
E_{xc}	: Exchange Correlation Energy
GF	: Green's Function
GGA	: Generalized Gradient Approximation
GMR	: Giant Magneto Resistance
LDA	: Local Density Approximation
LL	: Left Lead
MRAM	: Magnetic Random Access Memory
$n(r)$	: Ground state electron density
NEGF	: Non Equilibrium Green's Function Formalism
p	: Probability
RL	: Right Lead
spin FET	: Spin Field Effect Transistor
SWN	: Small world networks
TMR	: Tunneling Magneto Resistance
TPS	: Two Probe Systems
V_{eff}	: Effective potential
VNL	: Virtual Nano Lab

CHAPTER 1

INTRODUCTION

The purpose of this thesis is analyzing of structures composed of monatomic wires, containing the Carbon (C) atoms, by taking into account spin and charge properties of the electrons. The main aim is to examine the spin polarized transport through these structures, via calculation of transmission spectrum, conductance, spin polarized current, current-voltage characteristics, density of states, transmission eigenvalues and eigenstates etc. We also consider the effects of substitutional impurities in these nanostructures on spin polarized transport properties. To consider the behavior of spin dependent transport and calculation of spin polarized quantities, *Density Functional Theory* (DFT) based *Atomistix ToolKit* (ATK) software package was employed. The ATK is a *first-principles* simulation software which yields information in detail about the transport and electronic structure properties of nanoscale materials through the *Non Equilibrium Green's Function Formalism* (NEGF) and DFT. Applying this software one can establish molecular and bulk systems, two-probe systems (TPS) (Device configuration where the system is placed between electrodes) with a gate potential and get spin polarized properties under a bias voltage. We can also visualize the electron density, transmission eigenstates and band structure of the systems. The ATK can evaluate quantum mechanical equations describing electronic properties of nanoscale structures and model electronic structure and transport properties.

In this work, nanoscale structures composed of C monatomic wires are regarded as *Small World Networks* (SWN), a network between ordered and disordered systems. Structures, with different impurity concentrations and geometry, i. e. distinct

configurations, were analyzed. Upon understanding the mechanism governing the spin polarized transport, spin dependent properties of these structures were revealed.

This thesis is divided into 5 parts. We give a brief introduction of the theory in Chapter 2 and numerical method is introduced in Chapter 3; Spin Polarized Transport through Carbon Wires is presented in Chapter 4; Results and Discussions are given in Chapter 5.

CHAPTER 2

THEORETICAL BACKGROUND

2.1 DENSITY FUNCTIONAL THEORY (DFT)

DFT is a ground-state theory in which the emphasis is on the charge density as a relevant physical quantity [1]. DFT is one of the most successful approach for the description and computing of the electronic structure of metals, semiconductors and insulators. Its applicability ranges not only encompasses standard bulk materials but also complex materials, quantum and classical fluids. DFT is computationally very simple and allows to describe an interacting system fermions via its density.

For an *N* electron system, many-body Schrödinger equation is given as

$$\left[-\frac{\hbar^2}{2m}\sum_{i=1}^{N}\nabla_i^2+\sum_{i=1}^{N}v_{ext}(r_i)+\frac{1}{2}\sum_{i\neq j}\frac{e^2}{|r_i-r_j|}\right]\Psi(r_1,\dots,r_N)=E\Psi(r_1,\dots,r_N) \qquad (2.1)$$

where the first term is the kinetic energy of the nuclei, the second is the Coulomb interaction between the nuclei and each electron, the third term is the interaction energy between different electrons, $\Psi(r_1,\dots,r_N)$ is the many-body wave function and E is the total energy. Solving this equation exactly is impossible, thus other descriptions or approximations are required.

2.1.1 The Hohenberg-Kohn Theorem

The Hohenberg Kohn Theorem [2] points out that the density may be used in place of the potential as a basis function uniquely characterizing the system. The theorem shows that the ground state electron density $n(r)$ can expresses any ground state property and is sufficient to determine all the physical properties of the system. $n(r)$ is defined as

$$n(r)=N\int|\Psi(r,r_2,\dots,r_N)|^2\,dr_2\dots dr_N \qquad (2.2)$$

The ground state charge density also defines the ground state energy functional $E[n(r)]$:

$$E[n(r)] = \langle \Psi | T + U + V | \Psi \rangle = \langle \Psi | T + U | \Psi \rangle + \langle \Psi | V | \Psi \rangle = F[n(r)] + \int n(r)\, V_{ext}(r) dr \quad (2.3)$$

The internal energy functional $F[n(r)]$ is independent of the potential $V_{ext}(r)$ and it is described as follows:

$$F[n] = min_{\Psi \to n} \langle \Psi \left| \hat{T} + \hat{V}_{\infty} \right| \Psi \rangle \quad (2.4)$$

where $\hat{T}$ is a kinetic energy operator

2.1.2 The Kohn-Sham Theorem

In 1965, DFT was reformulated by Kohn and Sham (KS) [3]. Solution of the KS equations introduces the exact non-interacting kinetic energy, which includes almost all the true kinetic energy. KS demonstrated that the total ground state energy functional can be written as:

$$E[n(r)] = \left[T_{ni} + \frac{1}{2} \iint \frac{n(r) n(r')}{|r - r'|} dr dr' + E_{XC}[n(r)] + \int n(r) V_{ext}(r) dr \right] \quad (2.5)$$

here the first term is the kinetic energy of the non-interacting electron gas, the second term denotes the interaction between electrons, the third term is the exchange correlation term and the last one represents interaction between electrons and nuclei.

The one particle KS equation is:

$$\left[-\frac{\hbar^2}{2m} \nabla^2 + V_{eff}(r) \right] \Phi_i(r) = \epsilon_i \Phi_i \quad (2.6)$$

where Φ_i is KS orbitals, V_{eff} is the effective potential which is given by:

$$V_{eff} = V_{ext}(r) + e^2 \int dr' \frac{n(r')}{|r - r'|} + \frac{\delta E_{xc}[n]}{\delta n(r)} \quad (2.7)$$

where $n(r) = \sum_{i=1}^{N} |\Phi_i(r)|^2$. Thus, the external potential, the Hartree interaction and the exchange correlation potential form the effective potential.

The KS equation has to be solved self-consistently. The total electron density is the same as for the real system. However the KS orbitals have different physical meaning. The

eigenvalue of the highest occupied KS orbital is the first ionization potential for the exact density functional [4].

2.1.3 Approximations of the Exchange Correlation Energy Functional ($E_{xc}[n(r)]$)

As mentioned above, the number of variables is reduced through the DFT and KS equations. But the major problem is that the exact functional for exchange correlation $E_{xc}[n]$ is not known. If there is information about $E_{xc}[n]$, one can solve for the exact ground state energy and density. There are several ways of finding this functional. Here, the two most widely used are given namely the Local Density Approximation (LDA) and the Generalized Gradient Approximation (GGA).

2.1.3.1 Local Density Approximation (LDA)

In the LDA [5], the functional depends only on the density at the coordinate where the functional is evaluated:

$$E_{xc}^{LDA}[n] = \int \varepsilon_{xc}[n(r)]n(r)dr \qquad (2.8)$$

here E_{xc} is derived from the knowledge of the exchange-correlation energy per particle, ε_{xc}. Although covalent bonds, metallic bonds and ionic bonds are well described, LDA is not enough for the hydrogen bonds. In the LDA, $\varepsilon_{xc}[n(r)]$ is assumed to be homogenous at every point in the system even if the real charge density is not homogenous, which results in some errors.

2.1.3.2 Generalized Gradient Approximation (GGA)

GGA [6] uses the LDA and includes the gradient of the density at the same coordinate. In GGA, the exchange-correlation energy can be written as:

$$E_{xc}^{GGA}[n] = \int f[n(r), \nabla n(r)]n(r)dr \qquad (2.9)$$

where $f[n(r), \nabla n(r)]$ is a functional. Using the GGA, sufficiently good results have been achieved for molecular geometries and ground-state energies. The meta-GGA [7, 8] functional is more accurate than the GGA functional. This functional includes the Laplacian of the density.

2.2 GREEN'S FUNCTION (GF) FORMALISM

The single-particle GF operator $\hat{G}(E)$ of a system can be described as the solution of the operator equation,

$$\left[E - \hat{H}\right]\hat{G}(E) = 1 \tag{2.10}$$

A formal solution for this equation is given by $\hat{G}(E) = \left(E - \hat{H}\right)^{-1}$. If the variable *x* includes both the position and spin, $x = (r, \sigma)$, this equation becomes

$$[E - H(x)]G(x, x', E) = \delta(x - x') \tag{2.11}$$

where the GF is defines as $G(x, x', E) = \langle x\left|\hat{G}(E)\right|x'\rangle$.

Actually, the GF is a wave function at *r* resulting from a unit excitation at *r′*. Thus, it can also be considered as a source of an excitation. Because of the fact that the solution of Equation (2.11) is not well defined for values of *E* corresponding to the eigenvalues of the Hamiltonian, one must introduce an extra parameter (η), which yields retarded (G^+) and advanced (G^-) GF: $G^{\pm}(x, x', E) \equiv \lim_{\eta \to 0^+} G(x, x', E \pm i\eta)$.

Then equation (2.11) becomes

$$[E \pm i\eta - H(x)]G^{\pm}(x, x', E) = \delta(x - x') \tag{2.12}$$

$G^+$and G^- operators are defined uniquely for all real values of *E* by the relation:

$$\hat{G}^{\pm}(E) \equiv \lim_{\eta \to 0^+} \frac{1}{E \pm i\eta - \hat{H}} \tag{2.13}$$

2.2.1 NON EQUILIBRIUM GREEN'S FUNCTION FORMALISM (NEGF)

The NEGF formalism gives a microscopic theory for quantum transport containing interactions [9, 10]. The number of electrons *N* is described in terms of the density of states $D(E)$:

$$N = 2\int_{-\infty}^{\infty} dE D(E) \frac{\Gamma_1 f(E,\mu_1) + \Gamma_2 f(E,\mu_2)}{\Gamma_1 + \Gamma_2} \tag{2.14}$$

where $D(E) = \frac{1}{2\pi} \frac{\Gamma}{(E-\epsilon)^2 + \left(\Gamma/2\right)^2}$ with Γ being broadening matrix, which is also included in GF:

$$G(E) = \left(E - \epsilon + i\frac{\Gamma_1+\Gamma_2}{2}\right)^{-1} \quad (2.15)$$

Applying the spectral function $A(E) = -2\mathrm{Im}\{G(E)\}$ and the definition $D(E) = \frac{A(E)}{2\pi}$, N can be rewritten as:

$$N = \frac{2}{2\pi}\int_{-\infty}^{\infty} dE\left(|G(E)|^2\Gamma_1 f(E,\mu_1) + |G(E)|^2\Gamma_2 f(E,\mu_2)\right) \quad (2.16)$$

In the NEGF method, the GF is obtained by electronic structure of the contacts with the self energies and the details of the Hamiltonian of the scattering region:

$$G(E) = \lim_{\eta\to 0}[(E + i\eta) - H_s - \Sigma_1 - \Sigma_2]^{-1} \quad (2.17)$$

The left and right self energies Σ_1 and Σ_2 determine the effect of the leads and the interaction on the electron dynamics. Self energies are dependent of matrices, which include electronic structure of the right and left lead and their coupling to the scattering region. The two terminals current *I* including the broadening matrix is given as:

$$I = \frac{e}{h}\int_{-\infty}^{+\infty} dETr[G(E)\Gamma_1(E)G^{\dagger}(E)\Gamma_2(E)][f_1(E) - f_2(E)] \quad (2.18)$$

The density matrix ρ is can calculated from the GF of the scattering region:

$$\rho = \frac{1}{2\pi}\int dE\, G(E)[\Gamma_1(E)f_1(E) + \Gamma_2(E)f_2(E)]G^{\dagger}(E) \quad (2.19)$$

The NEGF and Landauer-Buttiker (LB) formalism have different properties. The NEGF centers on the internal state of a conductor, whereas in the Landauer approach, the internal state of the conductor does not appear.

2.3 LANDAUER BUTTIKER (LB) FORMALISM

Relation between the conductance and transport property in one dimension system was defined by Rolf Landauer in 1957 [11, 12]. The LB theory of transport demonstrates the method in order to describe the transport in mesoscopic systems, where the system size is crucial in determining the conductance.

The LB relates the linear conductance to the transmission and reflection probability at the Fermi energy. The formalism explains conductance in terms of static scattering properties. In conductors existence of impurities induces scatterings of incident electrons, resulting in a fraction of transmitted electrons. The transmitted fractions are called transmission coefficients. The current through a sample is connected to the probability of an electron to transmit through the sample. As stated above, central region of the device is attached to the leads that supply electrons from the electron reservoirs. In this formalism, the current flowing through the leads is given by:

$$I = \frac{g_s e}{h} \int_{E_{F_2}}^{E_{F_1}} D\,(E) f'(E) T(E) dE \qquad (2.20)$$

where $g_s = 2$ is the spin degeneracy, e is the electron charge, E_{F_1} and E_{F_2} are the Fermi levels of the left and right reservoirs, respectively. $f'(E)$ is the deviation from the equilibrium electron distribution, $T(E)$ is the transmission coefficient of electrons. The conductance G is defined by the current:

$$G = \frac{I}{V} = \frac{e^2}{\pi\hbar} T \qquad (2.21)$$

where V is the bias voltage. This relation between the conductance and the transmission is frequently used as the basis of understanding the transport in mesoscopic systems.

The potential drop related to the resistance (inverse of the conductance) occurs at the interfaces and the potential energy difference between the Fermi levels is given as

$$eV = E_{F_1} - E_{F_2} \qquad (2.22)$$

2.4 QUANTUM TRANSPORT

2.4.1 Ballistic Transport

Particles travel elastically through the central region without losing energy in ballistic transport. The central region can be defined by a scattering matrix approach proposed by Landauer that employs the transmission and reflection of the incoming waves at both sides. LB formalism is the best approach to express the transport that takes the spin up and spin-down current separately.

Consider a one dimensional wire coupled to the electrodes at zero temperature with chemical potentials μ_L and μ_R, through which the applied bias ΔV is given by $e(\mu_L - \mu_R)$[13]. If $\Delta V > 0$, the electrons flow from the filled states of the left electrode (L) to the empty states of the right electrode (R), along the wire, induce the following current (*I*),

$$I = (-e)(\mu_L - \mu_R)(v\frac{dn}{d\mu}) \tag{2.23}$$

where *v* is the Fermi velocity in the wire and $\frac{dn}{d\mu}$ is the density of states at the Fermi surface. As there are two spin species, density of states becomes $\frac{dn}{d\mu} = \frac{2}{hv}$. Another physical quantity is the conductance G. For a perfectly conducting one dimensional wire it is describing as

$$G = \frac{I}{\Delta V} = \frac{2e^2}{h} \tag{2.24}$$

For multiple conducting channels, a system with *n* channels, it becomes

$$G = \sum_{i=1}^{n}(T_i\frac{2e^2}{h}) \tag{2.25}$$

where T_i is the transmission coefficient for each channel.

2.4.2 Length Scales

In quantum transport, there are several characteristic lengths defining the low dimensional systems [14].

Mean free path(L_m), is a characteristic length described as the average path between the collisions with impurities. An electron moves in a perfect crystal like it is in the vacuum. If the crystal has impurities there are collisions and electrons are scattered from one state to another, resulting in momentum change. Therefore the distance that an electron travels until its momentum is unchanged is the mean free path. It is described as $L_m = v_f T_m$, where v_f is the Fermi velocity and T_m is the momentum relaxation time.

Phase-relaxation length (L_φ), is a quantum mechanical length that an electron travels before its initial phase is destroyed. The phase is important in the interference phenomena, where the wave functions of electrons having different pre-history are collected at the same

point. If the phases of the waves are not destroyed, specific quantum interference phenomena can be observed. The phase relaxation time (T_φ) describes the time concerning the relaxation of the phase memory. Scatterings against the static spin-independent potentials cannot lead to the phase relaxation. It may arise from electron-electron interactions, impurity etc. Phase relaxation length is given by $L_\varphi = v_f T_\varphi$.

De Broglie wave length (λ) is a length defined by $\lambda = \frac{2\pi\hbar}{p} = \frac{2\pi}{k}$ and for Fermi gas it is given by $\lambda_F = \frac{2\pi}{k_F}$, where k_F is the wave number at the Fermi level. In any system, the current is carried mainly by those electrons that have energies close to the Fermi energy at low temperatures. Thus, the relevant wavelength is λ_F.

2.5 SPINTRONICS

Spintronics or spin electronics is a field concerning spin-polarized transport in metals and semiconductors [15, 16]. The goal of spintronics is to find effective ways of controlling electronic properties by spin or magnetic field and to control spin or magnetic properties by, for instance, gate voltages. Spintronics is a study of spin phenomena in solids that is characterizing electrical, optical and magnetic properties of them in the presence of equilibrium and non-equilibrium spin populations. These studies give important insights about the nature of spin interactions (spin-orbit, hyperfine etc.) in solids, topological aspects of mesoscopic spin-polarized current in low-dimensional systems. It also ensures to examine microscopic mechanisms of magnetic long-range order and the electronic band structure in spin-polarized transport.

Electron is a particle with negative electric charge and half spin. The current electronics uses charge of electrons for storage, processing of information and in manipulating the electrons. Spin is neglected in electronics. On the contrary, magnetism uses spin properties of electrons and is used to develop materials. Spintronics or spin electronics is a field which employs both the charge and the spin property of the electrons. It combines electronics and magnetism. By taking advantage of the electron's spin degrees of freedom, there are, and will be, significant improvements in charge-based microelectronics in operating speed and power consumption. Spintronic devices have potential to replace the various conventional electronic devices with improved performance. The performance of spintronics

mainly depends on the spin polarization. Proposed schemes for spintronic devices generally require three essential elements [17]:

I. a mechanism for *electrically injecting* spin-polarized electrons into materials
II. a practical means for *spin manipulation* and transport
III. an electronic scheme for *detecting* the resulting spin polarization

2.6 SPINTRONICS BASED DEVICES

The common goal in many spintronics devices [18, 19] is to maximize the spin detection sensitivity to the point that it detects not the spin itself, but changes in the spin states. Today's research on spin electronics involves virtually all material families. The most advanced ones are the studies on magnetic multilayers. The first study concerning the spintronics is taken as the work by Albert Fert and Peter Grünberg. In this work, systems were shown to exhibit giant magneto resistance (GMR) [20, 21]. The idea is to increase the sensitivity of the electrical current due to magnetization changes. The GMR effect occurs in a nonmagnetic conductor sandwiched between two ferromagnetic layers. If the magnetizations of the two layers are parallel, the resistance is small and if they are antiparallel, it is large. The GMR devices have been successfully applied since 90s, in reading heads and high-density hard-discs.

Some other studies in spintronics are the tunneling magneto resistance (TMR) [22, 23] and spin transistor [24] in semiconductor spintronics. A metallic TMR is being employed as a non-volatile magnetic random access memory (MRAM). There have been some spin transistors proposed. One of them is the spin metal-oxide-silicon field-effect transistor (spin MOSFET) [25, 26]. This device acts as a spin valve [27] containing ferromagnetic electrodes. If the magnetizations of the ferromagnetic source and drain are parallel, the transport channel becomes open (ON); if the magnetizations are antiparallel, the channel gets closed (OFF). Another one is the spin field effect transistor (spin FET) proposed by Datta and Das, so known as Datta-Das spin transistor, in 1990 [24]. This design utilize the Rashba spin-orbit coupling [28] for its operational principle. The spin FET is a kind of TPS, where the transport channel, the CR, is a two-dimensional electron gas, LL and RL (source and drain, respectively) are ferromagnetic materials. In conventional field-effect transistors, the current

is due to the fact that the gate controls the channel through the electron concentration. But in spin FET the behavior of current is controlled by the gate which yields spin manipulation through Rashba spin-orbit coupling.

The Johnson spin switch was proposed as an all-metal Ohmic transistor [29]. It is based on spin-valve geometry. In the device, the nonmagnetic layer offers an additional contact. The magnetic bipolar transistor [30] is based on the design of conventional junction transistors. Owing to the spin-dependent tunneling across the emitter-base contact, it allows for spin-control of current amplification.

2.7 SMALL WORLD NETWORK (SWN)

SWN is a system between regular lattices and random ones. It is defined as being graphs that exhibit high clustering coefficient (like regular lattices) but low diameter (like random graphs) [31]. This model was suggested to grow a random graph while keeping its diameter small (see Figure 2.2). To this end one starts from a regular lattice and, through a probability *p*, rewires it, one edge after another, until a random graph is achieved. During this process, the farther the node being reconnected the more the graph diameter is reduced. After only a few steps the diameter of the graph is reduced dramatically while its clustering coefficient remains large.

To understand the resulting networks, two parameters are taken into account [31]. One of them is the characteristic path length which is the length of the shortest path required to connect one node to another, averaged over all pairs of nodes. The other parameter is the clustering coefficient (*C*). This coefficient defines the average probability that two nodes with a mutual "friend" will be connected. In terms of these parameters, for a SWN, the characteristic path length is similar to but *C* is much larger than that of a random network.

SWN occurs in many real-world phenomena, including road maps, food chains, electric power grids, telephone call graphs, and social influence networks [32]. It has extensive uses in many areas; such as complex networks, communication networks, cellular networks, etc.

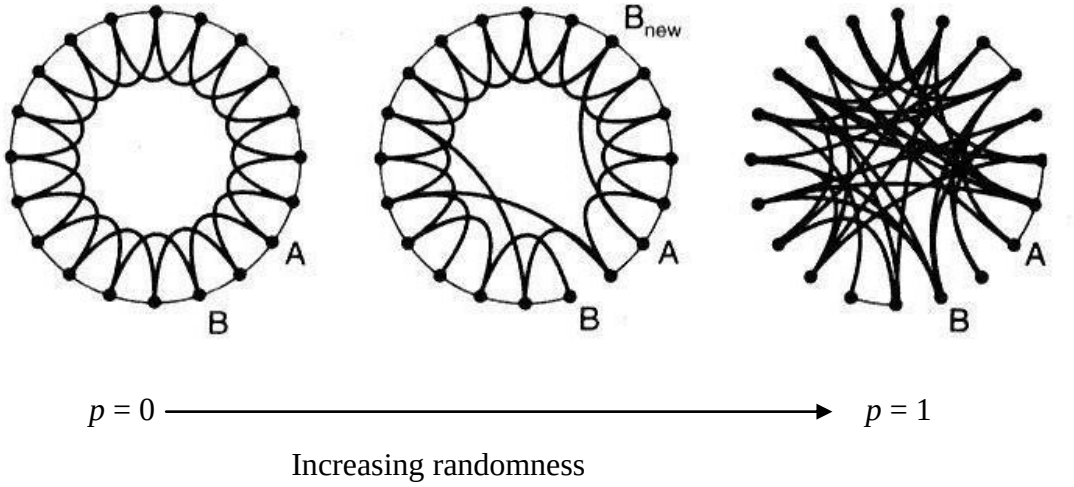

Figure 2.1: From regular to random networks [31]

2.8 WIRES COMPOSED of CARBON ATOMS

Molecular electronics have continually been improved since 1960 [33]. But some issues are still not clarified. Many theoretical and experimental studies have been performed on these problems. For example, linear gold chains suspended between two gold electrodes were produced [34]. A monatomic C linear chain has been observed at the center of multiwall C nanotubes [35]. They are ideal model systems for studying the electronic structures of low dimensional systems. C chains have robust electronic and mechanical properties. Interesting and potentially useful conductance variations can be achieved from them. Diamond crystal is a good insulator and in spite of it, an ideal C linear chain is a better conductor than gold chain. This exciting feature is due to the fact that C linear chain has double-bond formation between adjacent C atoms. Reactivity and flexibility of C chain allows structural and chemical variations. Although C linear chain is flexible, it has very high stiffness along the axial direction. One can construct pure or doped, finite or infinite, C chains with unusual properties, like ring, helix, grid and network structures. Number of C atoms in the system has influence on chemical, mechanical and transport properties of chains.

Some nano systems composed of C are believed to exist in the interstellar medium [36]. The size-dependent quantum effect of these nano-scale C systems is an important step toward their practical applications. They have potential applications in nano-science, molecular device design and astrophysics. Magnetism and quantum transport of C chains

have also attracted considerable attention for possible applications in spintronics, due to their remarkably long spin coherence time. Spin polarization in these systems may come from proximity to ferromagnetic metal [37, 38] or doped transition metals [39].

C nanotubes are the other type of systems comprising C atoms, which can be utilized in nanoscale electronic devices. Discovery of them [40] has stimulated many experimental and theoretical studies. C nanotubes are micron-long and nanometer-thick cylindrical shells of C. They have exciting special geometrical and electronic properties [41, 42]. They also have incredible strength and elasticity as well as extraordinary thermal and electrical conductivities. Since ballistic conduction nature and long spin scattering length exist in C nanotubes, they are considered to be promising spin mediators [43, 44].

CHAPTER 3

NUMERICAL METHOD

In numerical calculations, we have employed the software package ATK [45] to consider the spin dependent electrical transport properties of systems in atomic scales.

3.1 ATOMISTIX TOOLKIT (ATK)

ATK is a python script based interface which integrates a forceful scripting language and a graphical user interface. It is an extensive platform for studies in nanoelectronics and contains advanced electrostatic models to perform the realistic simulations of systems like nanoscale transistors. It is based on DFT combined with the NEGF, a development of the TranSIESTA-C code [46]. The ATK is able to perform calculations for many systems, including molecular, bulk and two probe systems (TPS). It also allows heterogeneous electrodes in investigating the transport properties of systems and supports for large scale simulations, over 1.000 atoms.

The ATK has very important calculation features, and so it is a digital engine. Some of the physical quantities that can be evaluated, concerning the spin polarized transport, are transmission spectrum, current, conductance, eigenvalues, eigenstates, scattering states, total energy, density of states, potential drop etc. In the calculations, an important ingredient is the approximation managed for the exchange correlation functional. The LDA and the GGA in the form of PBE exchange-correlation functional can be performed in ATK. Utilizing the spin-dependent exchange-correlation functionals, one can implement spin-polarized calculations.

3.2 VIRTUAL NANO LAB (VNL)

VNL is the graphical interface of ATK. It contains a set of modeling tools for studying nanoscale structures. One can perform calculations in VNL through the ATK, which is the engine of VNL. Transport properties and electronic structures of crystals, molecules, nanotubes, TPS (Device configuration) etc. can be modeled by the VNL.

Figure 3.1: The toolbar shows all the individual tools in VNL.

In VNL there are tools used to prepare the systems and perform the calculation. Some of them are:

Crystal Cupboard: It is the database of bulk crystals. During the construction of systems, crystal can be selected from here.

Atomic Manipulator: It sets up TPS upon properties of electrodes are defined. It is able to make modifications for magnetic tunnel junctions.

NanoLanguage Scripter: It contains calculation setup. Methods and parameters are adjusted in this tool.

Script Editor: It can be used to edit manually the scripts constructed by the different set of VNL tools.

The NanoLanguage Scripter tool is the main component used in the VNL for setting up calculations for the molecule, bulk and TPS. In this tool, the work-flow mainly involves the following steps: First of all, systems to be constructed are imported and prepared, via definition of parameters used in the calculations. Then physical quantities to be calculated are determined and calculation settings are saved as a script.

3.2.1 Two Probe System (TPS)

TPS are composed of three main parts: The central region (CR), where the systems are placed, left lead (LL, source) and right lead (RL, drain) (known as left and right electrodes). The CR is known as the scattering region which is located between LL and RL.

TPS may include identical (homogeneous) or distinct (heterogeneous) electrodes, which are semi-infinite leads connected to the reservoirs. Electrodes can be taken to be metallic lead, C or metal nanotubes with parallel or antiparallel spin polarizations. Electrodes must be periodic along the transport direction which is perpendicular to the interface plane, separating the CR from them. There shouldn't be interaction between the electrodes, i.e. they must not feel each other. Atoms in the LL cannot have any basis set overlapping with those in the RL. Electrodes can be long and wide enough to get more accurate results. During the calculation, electrodes can be taken as bulk, so that all interactions are taken into account.

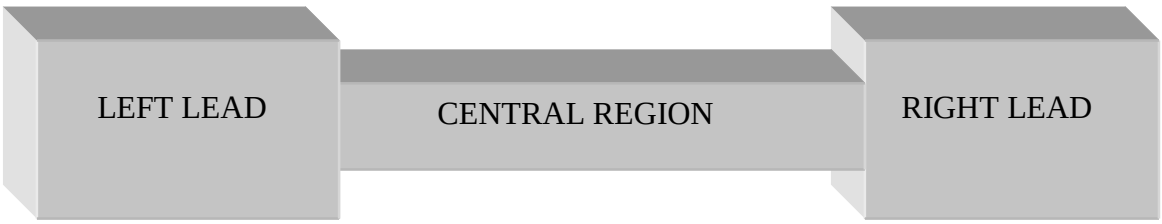

Figure 3.2: The TPS is composed of LL, CR and RL.

As stated, the region between the electrodes is called CR. In this part, one may have a molecule, a periodic structure or, for instance, a piece of C nanotube. It also contains some electrode atoms which are called as *screening* (surface) *layers*. These layers can be more than or equal to the electrode atoms defined in the unit cell. For a system resembling the real ones, it is crucial to note that surface layers cannot be shorter than the electrodes. Surface layers ensure screening, thus they reduce the effect of electrodes on the systems placed in the CR.

CHAPTER 4

CONSTRUCTION OF DISORDERED CARBON WIRES

Through ATK, we carried out simulations and calculations concerning the spin polarized transport properties for systems in the form of SWN composed of C atoms plus impurities. In these systems SWN are produced by C monatomic wires, yielding geometrically disordered systems. These systems may also contain impurity atoms. In order to generate SWN to be placed between left and right electrodes in TPS, we have written a code, named as "SWN Generator" (SWNG), in python as ATK is based on it. In this way one can able to construct complex systems, produced through a probability defined in SWN theory. As stated in the previous chapters, the electrode atoms are also included at the beginning and the end of the CR of TPS, screening region, in order to decrease the effect of the electrodes on the constructed system. The electrodes were chosen to contain either C or Ni atoms. The system to be considered includes C plus impurities both on the main chain and bonds.

There are some crucial distances required to be calculated before generating the SWN: Interatomic distance (lattice constant) in the central or scattering region; the distance between the electrodes and the system; the distance between the main chain and the bonds. Both lattice constant and electrode-system distance were obtained by minimization of the total energy. This minima in energy corresponds to the equilibrium lattice constant (a).

To analyze the systems by ATK we need to apply the TPS, which is produced in three steps:

- Construction of the electrodes,
- Setting up the central or scattering region,

- Combining the electrodes and scattering region into a single system (Device Configuration)

The electrodes are constructed by defining a proper the unit cell. The unit cell has three linearly independent vectors: S1, S2 and S3 along *x*, *y* and *z* axes, respectively. The S3 indicates the transport direction along which electrons are propagating. In this work, electrodes elongated into the central regions were in general formed as one-dimensional chain for C and taken thicker for Ni. We must ensure that the electrode unit cell becomes sufficiently large along S1 and S2 directions to inhibit the interactions.

In Figure 4.1 – 4.3, we have presented total energy - lattice spacing relationships for some simple monatomic systems we have utilized. As stated through the minima we have found the *a*.

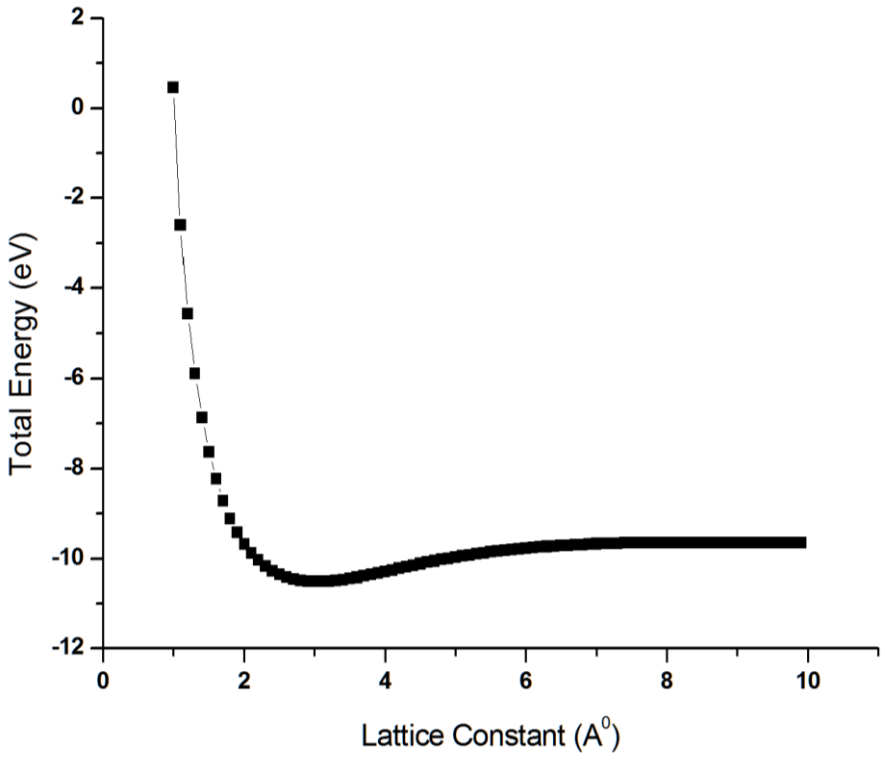

Figure 4.1: Total energy – lattice spacing graph for Li monatomic chain (*a* = 2.90 Å).

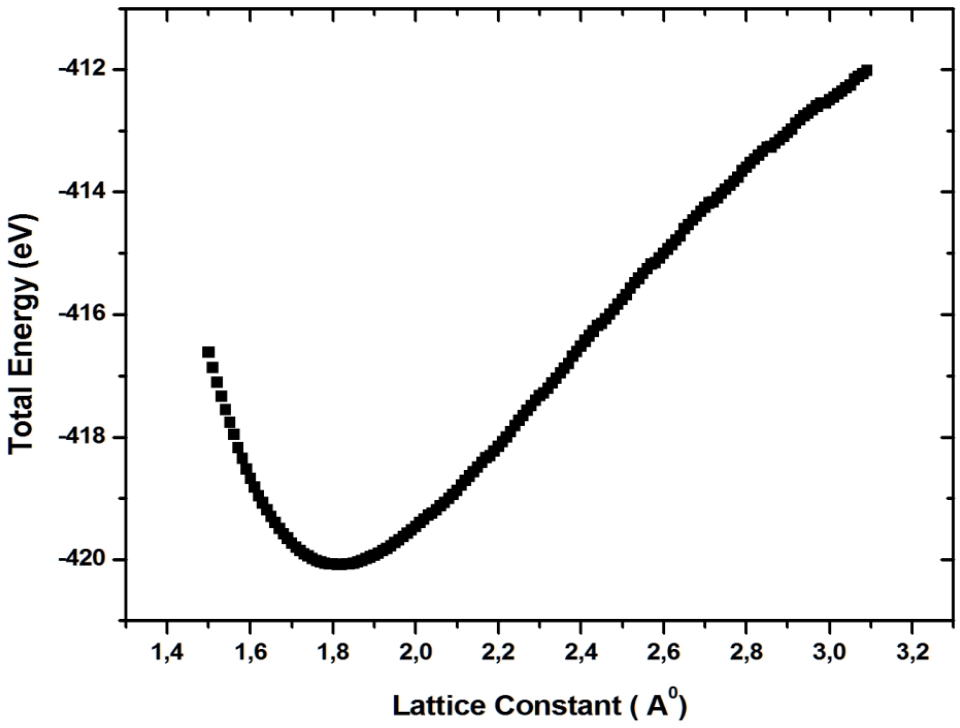

Figure 4.2: Total energy – lattice spacing graph for monatomic chain composed of C and Cr (a = 1.81 Å).

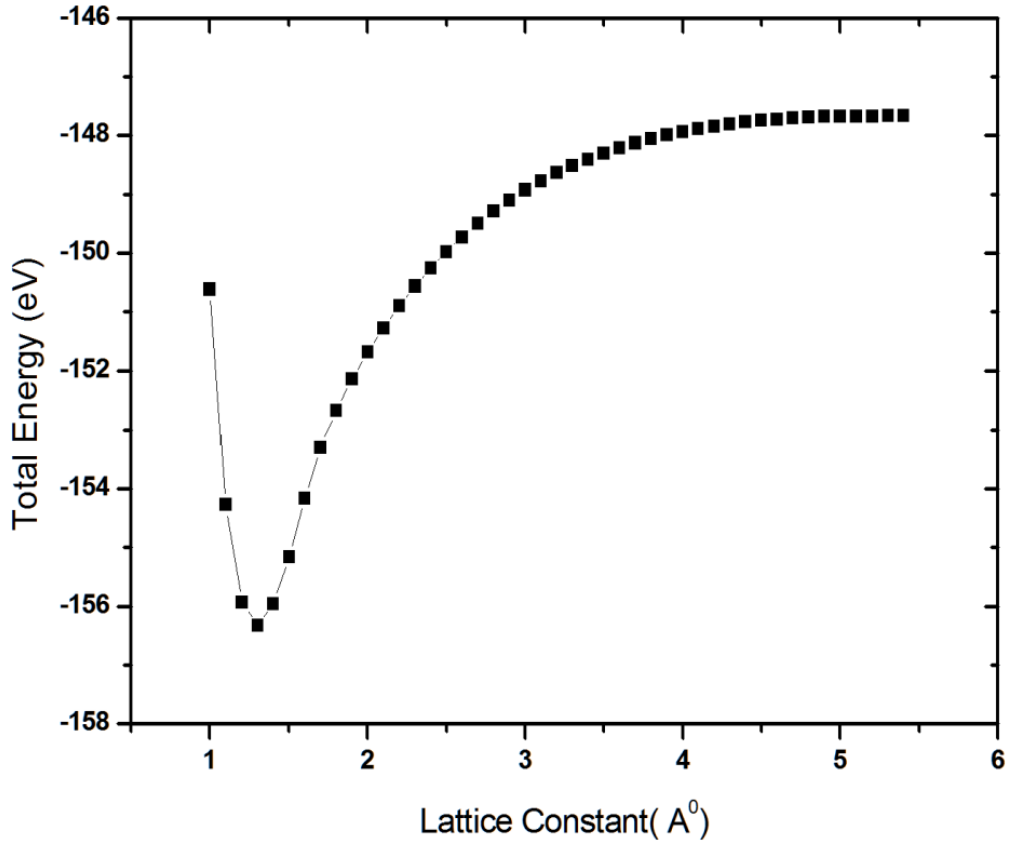

Figure 4.3: Total energy – lattice spacing graph for C monatomic chain (a = 1.40 Å).

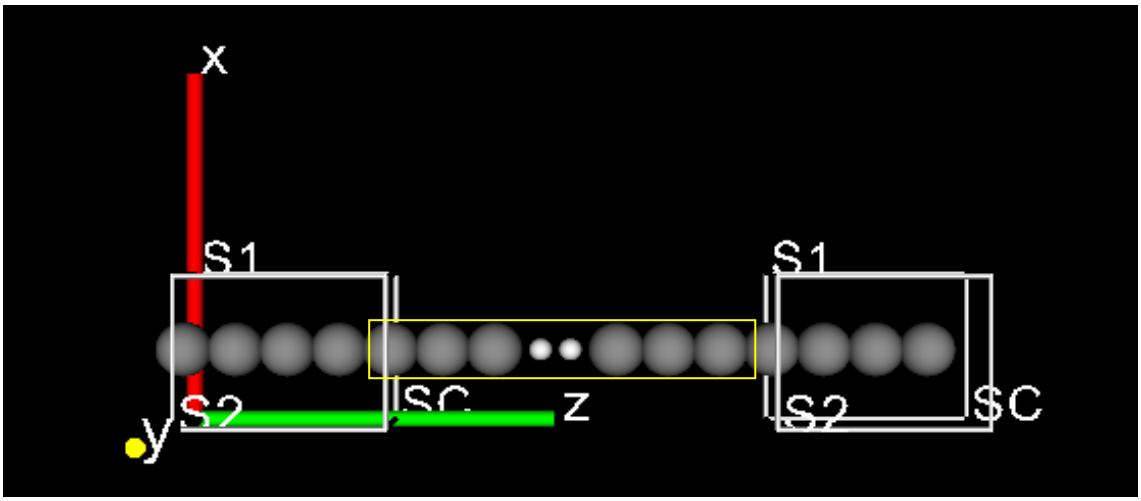

Figure 4.4: A simple TPS prepared in ATK. Here, the left and right white boxes indicate the unit cell of the electrodes that contain four C (grey) atoms. The yellow box stands for CR containing C and H (white) atoms.

In Figure 4.4, a simple TPS system is illustrated. It may be used to consider the effects of two H atoms on the transport. Here the H atoms are taken to be substitutional impurities which have crucial effects on the transport properties of the systems. The left and right part of the H atoms in the CR are the screening layers which are the elongated parts of the LL and RL. In this particular figure, the electrode unit cell contains four C atoms positioned in the middle of the cell. Thus, the length of it becomes 4 × 1.4 Å, since the C-C interatomic spacing is 1.4 Å.

As an example, the script below shows the details of steps for setting up the system in Figure 4.4.

```
from ATK.TwoProbe import *
# Cchain lattice constant
a = 1.40
# Construct the electrode unit cell
unit_cell = [ [3*a, 0.0, 0.0 ],
              [0.0, 3*a, 0.0 ],
              [0.0, 0.0, 4*a ] ] * Angstrom
```

```
# Define the electrode
        electrode_C = PeriodicAtomConfiguration(
                super_cell_vectors=unit_cell,
                elements= 4*[Carbon],
                fractional_coordinates=[(0.5, 0.5, float(i)/4.0) for i in range(0,4)])
        # Setup the two-probe scattering region
        dist_HH = 0.804
        dist_CH = 1.25
        # The atoms in the central region
        elements = 3*[Carbon] + 2*[Hydrogen] + 3*[Carbon]
        positions = [
                (0.0, 0.0, 0*a),
                (0.0, 0.0, 1*a),
                (0.0, 0.0, 2*a),
                (0.0, 0.0, 2*a + dist_CH),
                (0.0, 0.0, 2*a + dist_CH + dist_HH),
                (0.0, 0.0, 2*a + dist_CH + dist_HH + dist_CH + 0*a),
                (0.0, 0.0, 2*a + dist_CH + dist_HH + dist_CH + 1*a),
                (0.0, 0.0, 2*a + dist_CH + dist_HH + dist_CH + 2*a)] * Angstrom
        # Combine electrode and scattering region
        # into a two-probe system
        two_probe = TwoProbeConfiguration(
                electrodes = (electrode_C,electrode_C),
                scattering_region_elements = elements,
                scattering_region_cartesian_coordinates = positions)
        # Export the two-probe system to VNL file.
        vnl_file = VNLFile("ch2c.vnl")
        vnl_file.addToSample(two_probe, "ch2c")
```

In the CR (scattering region), the first and last atoms are attached to the last and first atom of LL and RL, respectively. After constructing this TPS, we can perform a self-consistent field (SCF) calculation for the system in CR. For the specific SCF calculations, we need to set some parameters, defined in ATK, such as basis set

parameters, Brillouin zone parameters, mesh-cut off etc. We usually choose the Double Zeta Polarized basis set, but basis set depends on configuration of systems and atom type. Depending on systems, GGA or LDA exchange correlation functions are preferred.

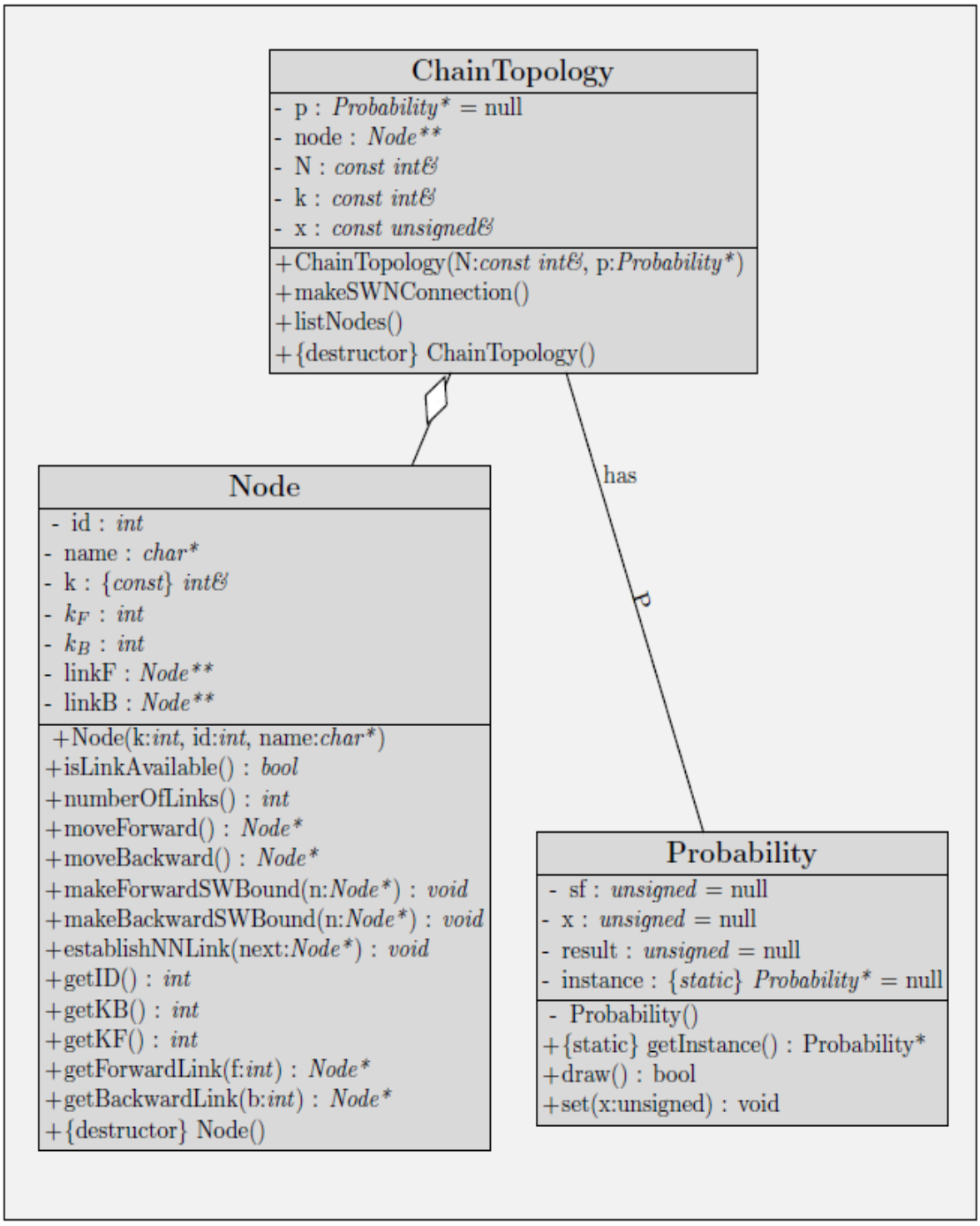

Figure 4.5: Class diagrams defined in SWNG.

4.1 SMALL WORLD NETWORK GENERATOR (SWNG)

In order to construct complex structures in the form of SWN using the SWN theory, we have developed a code, named as SWNG, in phython as ATK is based on it. SWNG yields topologically disordered systems as a result of probability defined in SWN theory. After producing the systems in SWNG, they are integrated into ATK using TPS to investigate the spin polarized transport properties of them.

4.1.1 Class Diagrams for SWNG

These diagrams give the SWN topology due to the nodes on the main chain and probability, by which bonds are inserted and distributed (see Figure 4.5). A node refers an atom in the system. Depending on the characteristics of a system, depending on atom type, number of links on a node may be changed. Each node is connected to its nearest neighbors and, randomly, to atoms on bonds. In Figure 4.5, the proper links described by class are shown.

4.1.2 Algorithm of SWNG

The algorithm of SWNG code, for a pure SWN system, is given in Figure 4.6. In this algorithm, N gives the total number of atoms of the system; k indicates the maximum possible neighbors for each atom (node) on the main chain; p is the probability described in SWN theory. The other parameters are already introduced in this figure. In Figure 4.7, an algorithm is presented. It is used to establish a bond between two specific atoms on the main chain.

```
Input: List of nodes: {1, 2, ..., N}; k: number of neighbors, p:
       probability: 0 < p < 1. It is assumed that initially all nodes have
       nearest neighbor connection.
Output: Small-World Network topology is generated with probability p.
ChainTopology :: makeSWNConnection() ;
begin
    foreach (n_i : nodes ∘ i = 1, 2, ..., N) do
        if {(n_i → k_F + n_i → k_B) < n_i → k} then
            Draw a SW bond with probability p;
            if {p is matched} then
                Choose randomly an end node from the list:
                j = 1 + (V ≠ 0) × j + rand()%{N − (V ≠ 0) × j};
                if {j ∉ {i − 1, i, i + 1}} then
                    if {(j − i) > 0} then
                        Move (j − i) steps forward via n_j → moveForward();
                        if {(n_j → k_F + n_j → k_B) < n_j → k} then
                            n_i → makeForwardSWBond(n_j);
                        end
                    end
                    if {(j − i) < 0} then
                        Move (j − i) steps backward via
                        n_j → moveBackward();
                        if {(n_j → k_F + n_j → k_B) < n_j → k} then
                            n_i → makeBackwardSWBond(n_j);
                        end
                    end
                end
            end
        end
        Increment index: i = i + 1;
    end
end
```

Figure 4.6: The algorithm of SWNG.

Input: The current node is initial node and a final node which is a forward node is given as a parameter.
Output: Making a small world bond between two nodes.
Node :: makeForwardSWBond(n_f);
begin
  this $\rightarrow$ link$_F$[**this** $\rightarrow k_F$] $= n_f$;
  $n_f \rightarrow$ link$_B$[$n_f \rightarrow k_B$] $=$ **this**;
  this $\rightarrow k_F + +$;
  $n_f \rightarrow k_B + +$;
end

Figure 4.7: An algorithm establishing a bond between initial node and a final node on the main chain.

Performing the SWNG we can construct SWN systems for desired probabilities. These probabilities result in topologically disordered systems composed of C atoms plus substitutional impurities. For instance one can get a system consisting of four bonds as shown in Figure 4.8. Here t_{ij}^{sw} is the hopping term, defined in tight-binding approximation, for the corresponding bond.

Figure 4.8: A SWN system having 4 bonds**.**

4.2 DISTRIBUTION OF SUBSTITUTIONAL IMPURITIES

The substitutional impurities are placed and distributed through a given probability. Gaussian, uniform and exponential distribution are utilized to locate the different kind of impurities. In Figure 4.9, there is an algorithm giving location of substitutional impurities using Gaussian distribution.

```
Input: List of randomly distributed numbers: {1, 2, ..., N}.
μ and σ are given.
Output: ....
begin
    i=1;
    while (i ≤ N_j) do
        n = 1;
        x_n = RN[n];
        draw = random.random() # 0 < draw < 1;
        cond=(gaussian(x_n − σ/2)≤ draw) & (draw ≤
        gaussian(x_n + σ/2));
        if cond then
            p_j : particles(j);
            insert(p_j, x_n);
            remove(x_n, RN);
            uniform_randomize(RN);
            n = n + 1;
            i = i + 1;
        end
    end
end
```

Figure 4.9: The algorithm to place the substitutional impurities using Gaussian distribution.

Depending on the distribution functions, there are four artificial ways to add the impurity particles on the main chain or bonds by replacing the host atoms in the pure system:

- Location of impurities on the main chain
- Location of impurities on an arbitrary bond
- Location of impurities on bonds without main chain
- Location of impurities on bonds plus main chain, i.e., insertion based on distribution function.

4.2.1 The Process of Inserting Impurities

Let's consider the process of inserting impurity particles on a system with a specified probability distribution. It is schematically presented in Figure 4.10. In this figure, $N = 8$ indicates the total number of atoms on the main chain; red circle is the C atom and the other circles represent the impurities which are Li and Au atoms. Based on

the distribution function, the impurities are located. Here there are 3 Li atoms and 2 Au atoms.

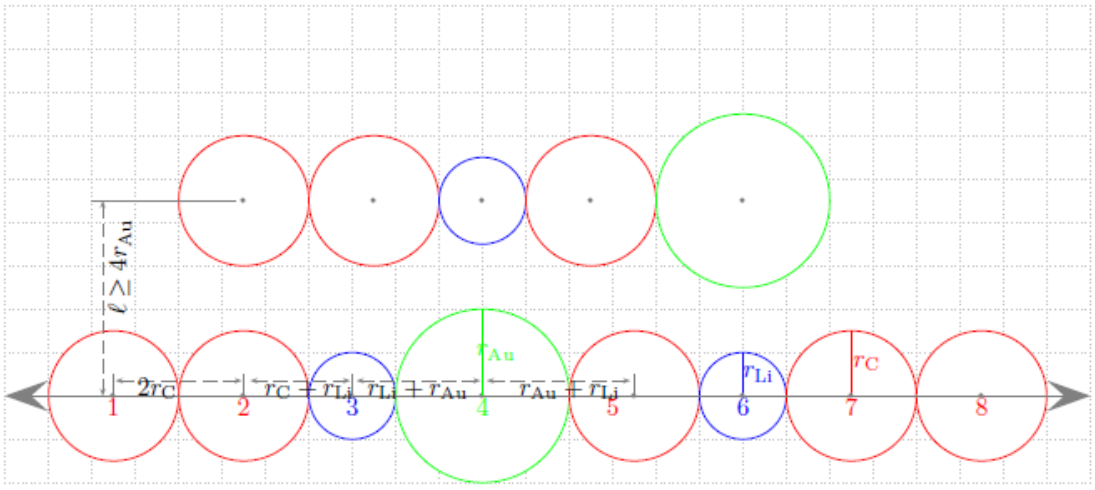

Figure 4.10: Distribution of impurities.

The distribution of impurities either to the main chain or bonds is acquired by the number of atoms on the main chain. Thus the number of impurities to be located on the bonds depends on length of main chain. In Figure 4.10, on the main chain, the number of Li atoms is $N_{\mathrm{Li}} = 2$ and that of Au atoms is $N_{\mathrm{Au}} = 1$. Among C atoms ($N_{\mathrm{C}} = 5$ on the main chain) they are distributed. The percentage of the impurities on the main chain is $x_{Li} = \frac{N_{Li}}{N} \times 100 = 25\%$ and $x_{Au} = \frac{N_{Au}}{N} \times 100 = 12.5\%$.

The perpendicular distance between main chain and bonds: In order to get rid of the overlapping between bonds and main chain, we must pay attention to the corresponding distance. The distance between bonds and the main chain must be adjusted such that no interaction takes place. To make such a setting we take into account the size of the largest particle in the system. We have observed that if one takes this distance to be approximately four times the radius of the largest particle then the interaction disappears. For instance, as shown in Figure 4.10, the largest particle is Au and the distance (l) must be $l \geq 4 \times r_{\mathrm{Au}}$.

4.2.2 Integration SWNG into ATK

Upon constructing the systems using SWNG, we have integrated them into ATK. Some representative SWN systems, constructed in this way, are shown in Figures 4.11 – 4.16. Here the SWN systems have been produced by the probabilities p = 0.1, 0.2 and 0.5.

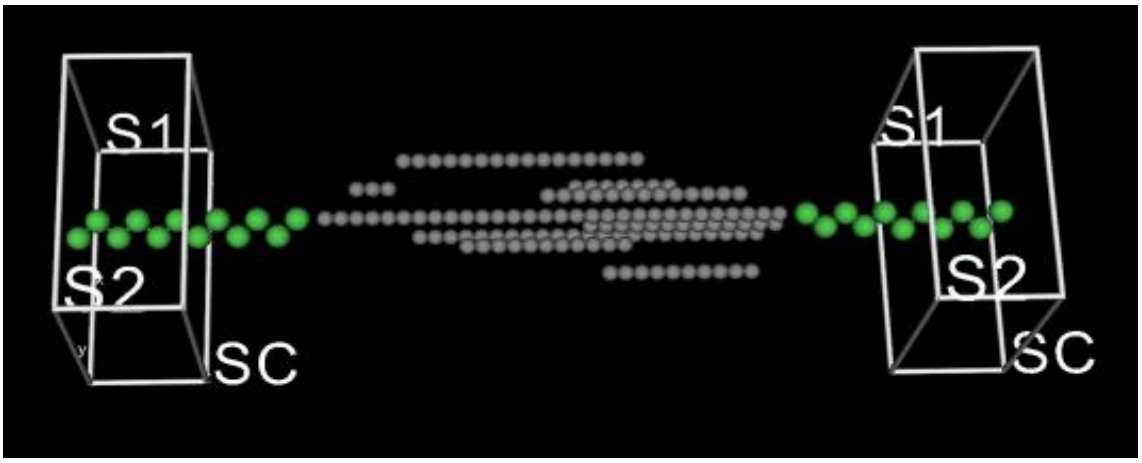

Figure 4.11: SWN composed of C monatomic wire plus 8 bonds between Ni electrodes (p=0.5).

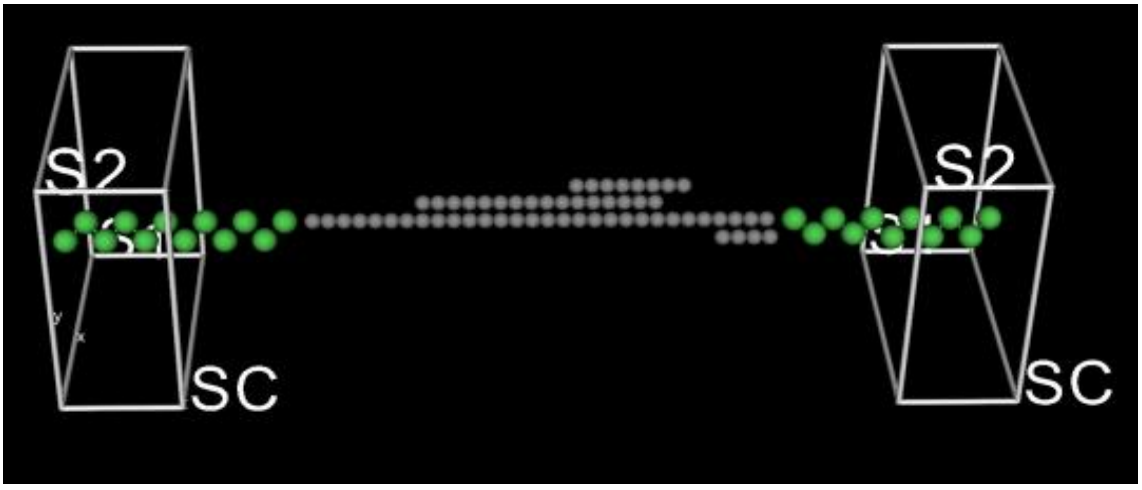

Figure 4.12: SWN composed of C monatomic wire plus 3 bonds between Ni electrodes (p=0.1).

We examined similar systems constructed by different probabilities, through SWNG, to see the effects of them on transport. Besides that we have inserted the same SWN systems between distinct electrodes to understand the influence of them. For the parallel and anti parallel spin polarized electrodes thick Ni atoms have been taken, otherwise monatomic C electrodes have been used.

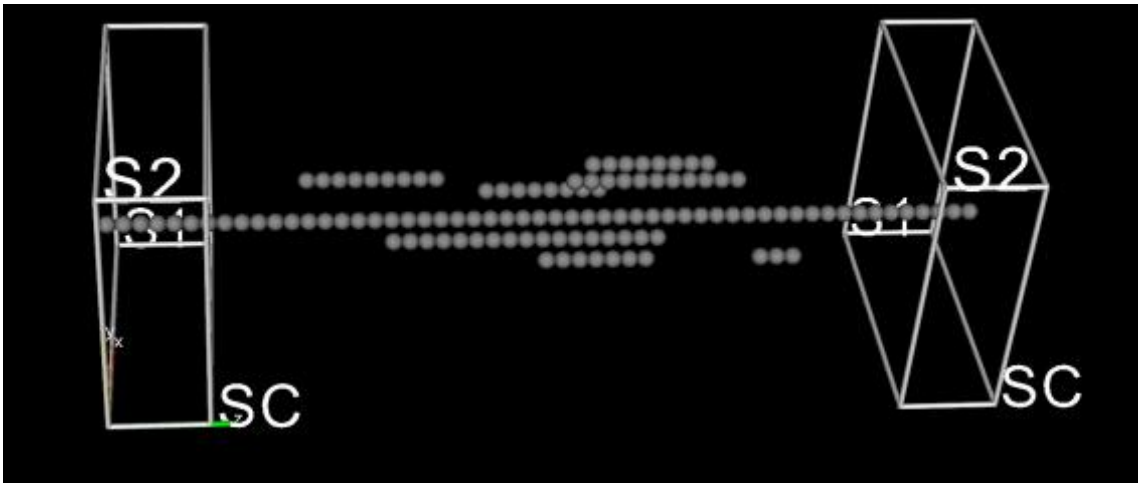

Figure 4.13: SWN composed of C monatomic wire plus 7 bonds between C electrodes (p=0.2).

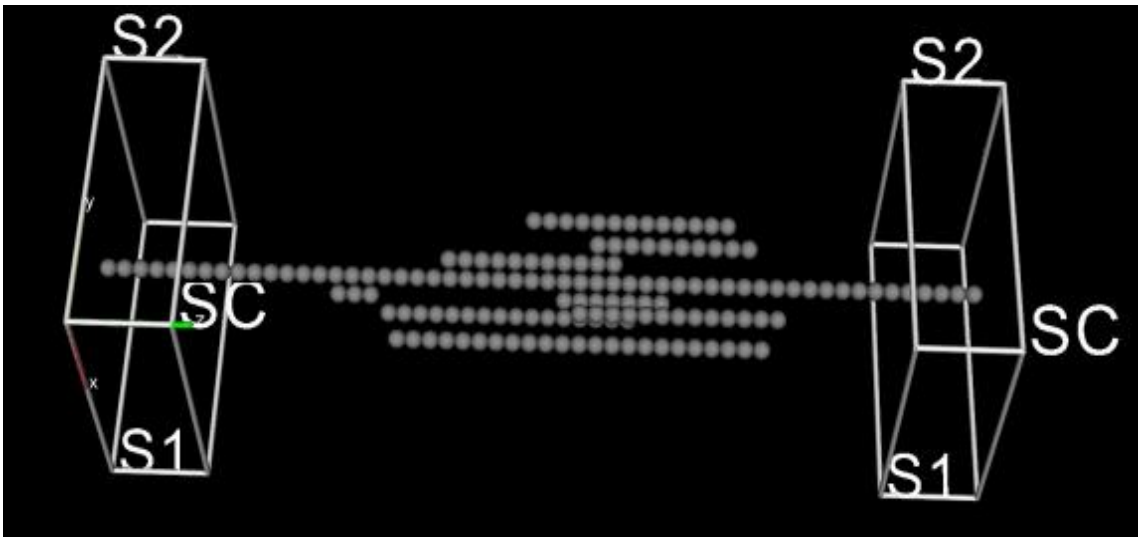

Figure 4.14: SWN composed of C monatomic wire plus 8 bonds between C electrodes (p=0.5).

Co, Cr and H atoms are taken as substitutional impurities. The same configurations with and without impurities are compared to see the effect of impurities. Two sample systems are given in Figure 4.15 and 4.16.

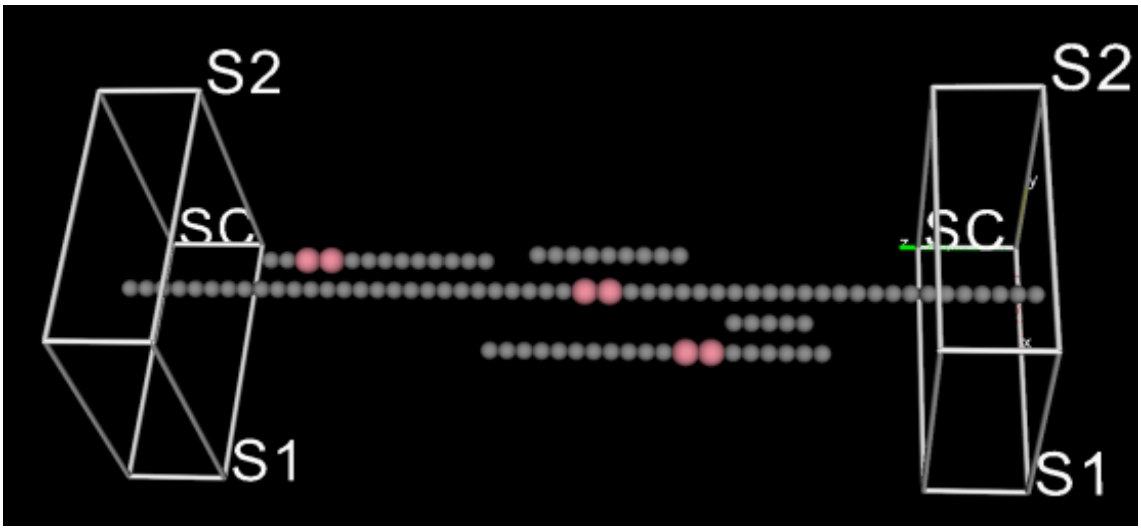

Figure 4.15: SWN composed of C monatomic wire plus 4 bonds and Co impurities between C electrodes (p = 0.1).

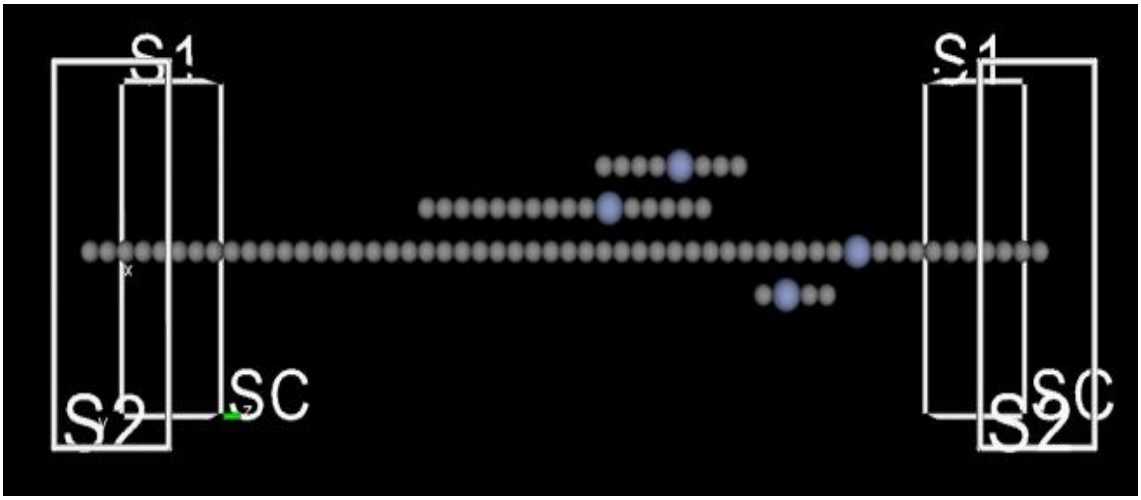

Figure 4.16: SWN composed of C monatomic wire plus 3 bonds and Cr impurities between C electrodes (p = 0.1).

CHAPTER 5

RESULTS AND DISCUSSIONS

We have constructed topologically disordered systems, composed of C atoms plus impurities, using SWNG we have developed as stated in the previous chapter. Spin polarized transport properties are investigated upon integrating the systems into ATK via TPS. We have found numerical results for transmission spectrum, current-voltage characteristics, conductance, density of states (DOS) etc.

In the following there is a representative script in which the calculation of transmission, total energy, density of states, conductance at the Fermi energy is given.

```
---------------------------------------------------------------------------------------------
from ATK.TwoProbe import *

scf = restoreSelfConsistentCalculation("C_script-scf.nc")
system="C_script_calc"
vnlfile = VNLFile(system + ".vnl")

import numpy
energy_list = numpy.arange(-5.0, 5.1, 0.05)*electronVolt
bz_int_param = brillouinZoneIntegrationParameters((1,1,100))

# Calculate transmission spectrum
trans_spectrum = calculateTransmissionSpectrum(
self_consistent_calculation = scf,
        energies = energy_list,
        brillouin_zone_integration_parameters = bz_int_param)
```

```
vnlfile.addToSample(trans_spectrum,'Transmission Spectrum')
energy = calculateTotalEnergy(scf)
print energy
vnlfile.addToSample(energy,'Total Energy')

# Calculate density of states
density_of_states = calculateDensityOfStates(
        self_consistent_calculation = scf,
        energies = energy_list)

vnlfile.addToSample(density_of_states,'Density of States')

t = density_of_states.energies()
dos = density_of_states.densityOfStates()

f = open('Dos-energy.dat', 'w')
f.write ('   Energy (eV) ')
f.write ('---------------')
for i in range(len(energy_list)):
        f.write ("%g\t%g\n" % ( t[i].inUnitsOf(eV),dos[i].inUnitsOf(eV**(-1))))
f.close()

# Define conductance quantum
conductance_quantum = 7.748091733e-5*Siemens

# Calculate transmission spectrum at E_Fermi
fermi_trans = calculateTransmissionSpectrum(
        self_consistent_calculation = scf,
        energies = [0.0]*electronVolt)
conductance = fermi_trans.coefficients()[0] * conductance_quantum
vnlfile.addToSample(conductance,'Conductance')
print conductance
```

In the script above, “C_script-scf.nc” is the DFT based SCF calculation determined for the corresponding system, already formed, which is restored. Here the considered system is spin independent, so there are not parameters related to spin. In the script below, calculation parameters are given to perform a SCF spin polarized calculation for a system consisting of C atoms inserted between Ni electrodes (Ni-C-Ni TPS system).

```
from ATK.TwoProbe import *
from ATK.MPI import processIsMaster
system='Ni-C-Ni'

#.....................Parameters.....................
parallel_spin=True
scf_kpoints=(5,5,50)
mesh_cutoff=150.*Rydberg
xc=LDA.PZ
temperature=1200.*Kelvin
tolerance=1e-005
basis_set_parameters = basisSetParameters(type = DoubleZetaPolarized)
diagonal_mixing_parameter = 0.05
history_steps = 7
max_steps = 200
integral_lower_bound = 7.0*Rydberg
circle_points = 50
path='/data1/clusterfs/users/fatma'
vnl_file=system +'.vnl'
verbosity=10
checkpoint_basename=system
if parallel_spin:
checkpoint_file=path + '/' + checkpoint_basename + '_up_up.nc'
else:
checkpoint_file=path + '/' + checkpoint_basename + '_up_down.nc'
```

```
#.....................................................................................

#.................Importing The Geometry.............................
vnlfile=VNLFile(path + '/' + vnl_file)
dict=vnlfile.readAtomicConfigurations()
twoprobe_configuration=dict[dict.keys()[0]]
#.....................................................................................
# The number of atoms in the electrode
num_Ni_atoms=len(twoprobe_configuration.electrodes()[0].elements())
# The number of atoms in the left and right surfaces
central_region_elements=twoprobe_configuration.elements()
num_Ni_surface_atoms=0
for atom in central_region_elements:
if atom==Nickel:
        num_Ni_surface_atoms +=1
else:
        break
# The number of C atoms in the central region
num_C_atoms=len(central_region_elements)-2*num_Ni_surface_atoms
#Initial spins
left_electrode_initial_scaled_spin=[1.0,]*num_Ni_atoms
central_region_initial_scaled_spin=[1.0,]*num_Ni_surface_atoms + \
                                   [0.,]*num_C_atoms
if parallel_spin:
central_region_initial_scaled_spin +=[1.0,]*num_Ni_surface_atoms
right_electrode_initial_scaled_spin =[1.0,]*num_Ni_atoms
else:
central_region_initial_scaled_spin +=[-1.0,]*num_Ni_surface_atoms
right_electrode_initial_scaled_spin =[-1.0,]*num_Ni_atoms

#####################################################################
#The Electrode Parameters
#####################################################################
left_electrode_parameters = ElectrodeParameters(
```

```
        brillouin_zone_integration_parameters=brillouinZoneIntegrationParamet
ers (scf_kpoints),
        electron_density_parameters = electronDensityParameters(
                mesh_cutoff = mesh_cutoff,
                initial_scaled_spin = left_electrode_initial_scaled_spin),
        iteration_mixing_parameters = iterationMixingParameters(
                diagonal_mixing_parameter = diagonal_mixing_parameter,
                history_steps = history_steps),
        iteration_control_parameters = iterationControlParameters(
                tolerance = tolerance,
                max_steps = max_steps),
        eigenstate_occupation_parameters = eigenstateOccupationParameters(
                temperature = temperature)
)

right_electrode_parameters = ElectrodeParameters(
        brillouin_zone_integration_parameters=brillouinZoneIntegrationParamet
ers(scf_kpoints),
        electron_density_parameters = electronDensityParameters(
                mesh_cutoff = mesh_cutoff,
        initial_scaled_spin = right_electrode_initial_scaled_spin),
        iteration_mixing_parameters = iterationMixingParameters(
                diagonal_mixing_parameter = diagonal_mixing_parameter,
                history_steps = history_steps),
iteration_control_parameters = iterationControlParameters(
                tolerance = tolerance,
                max_steps = max_steps),
        eigenstate_occupation_parameters = eigenstateOccupationParameters(
                temperature = temperature)
)

#Two-Probe Method
twoprobe_method = TwoProbeMethod(
```

```
        electrode_parameters=(left_electrode_parameters,right_electrode_param
    eters),
        exchange_correlation_type = xc,
    basis_set_parameters = basis_set_parameters,

        electron_density_parameters = electronDensityParameters(
            mesh_cutoff = mesh_cutoff,
        initial_scaled_spin = central_region_initial_scaled_spin),
    iteration_mixing_parameters = iterationMixingParameters(
            diagonal_mixing_parameter = diagonal_mixing_parameter,
            history_steps = history_steps),
    iteration_control_parameters = iterationControlParameters(
            tolerance = tolerance,
            max_steps = max_steps),
    energy_contour_integral_parameters= energyContourIntegralParameters(
            integral_lower_bound = integral_lower_bound,
        circle_points = circle_points),
    algorithm_parameters = twoProbeAlgorithmParameters(
            initial_density_type = InitialDensityType.NeutralAtom)
    )

    import ATK
    ATK.setVerbosityLevel(verbosity)
    ATK.setCheckpointFilename(checkpoint_file)

    # Perform self-consistent field calculation
    scf = executeSelfConsistentCalculation(
       twoprobe_configuration,
       twoprobe_method  )
```

5.1 NUMERICAL RESULTS

In this section we present the SCF results for some systems we examined. Both spin independent and spin polarized numerical calculation results are given.

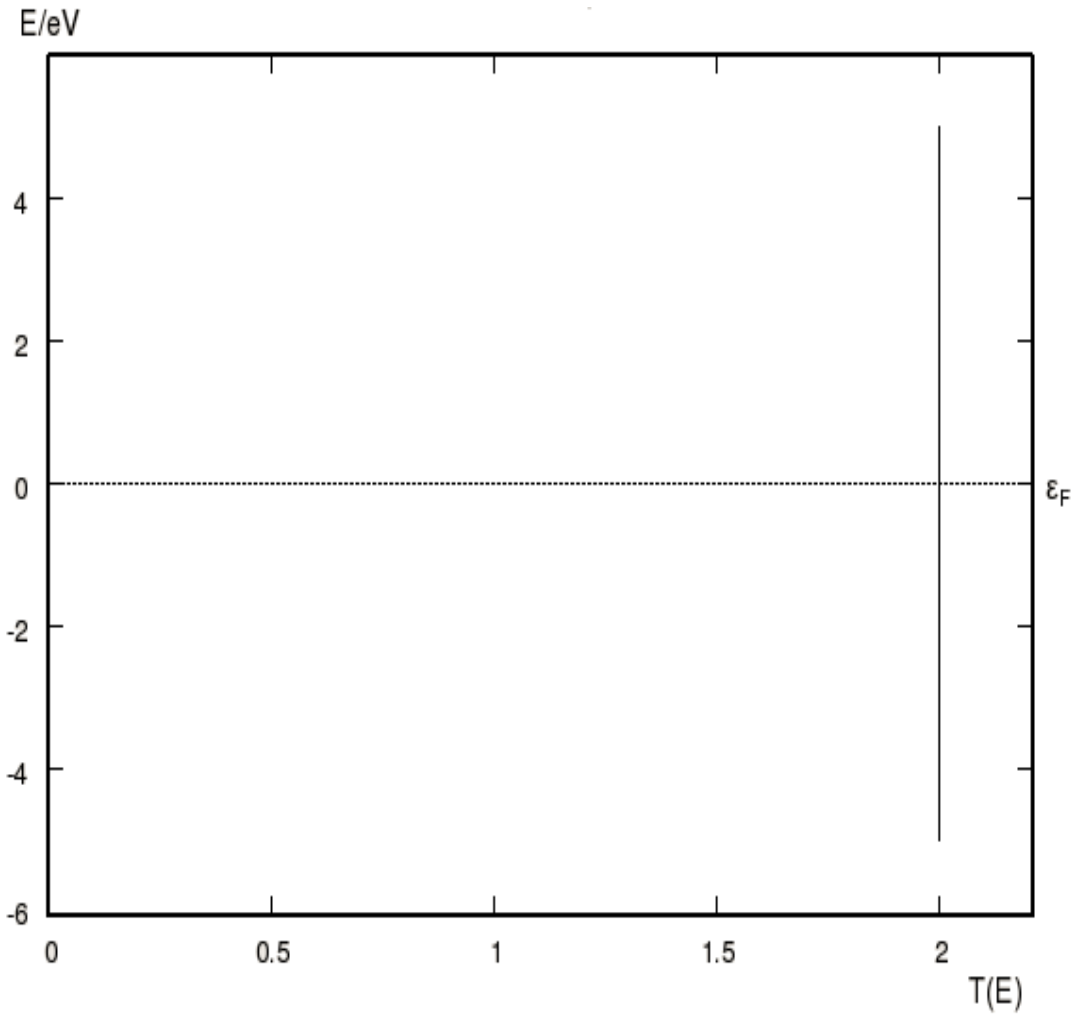

Figure 5.1: Transmission spectrum of a pure C chain without spin.

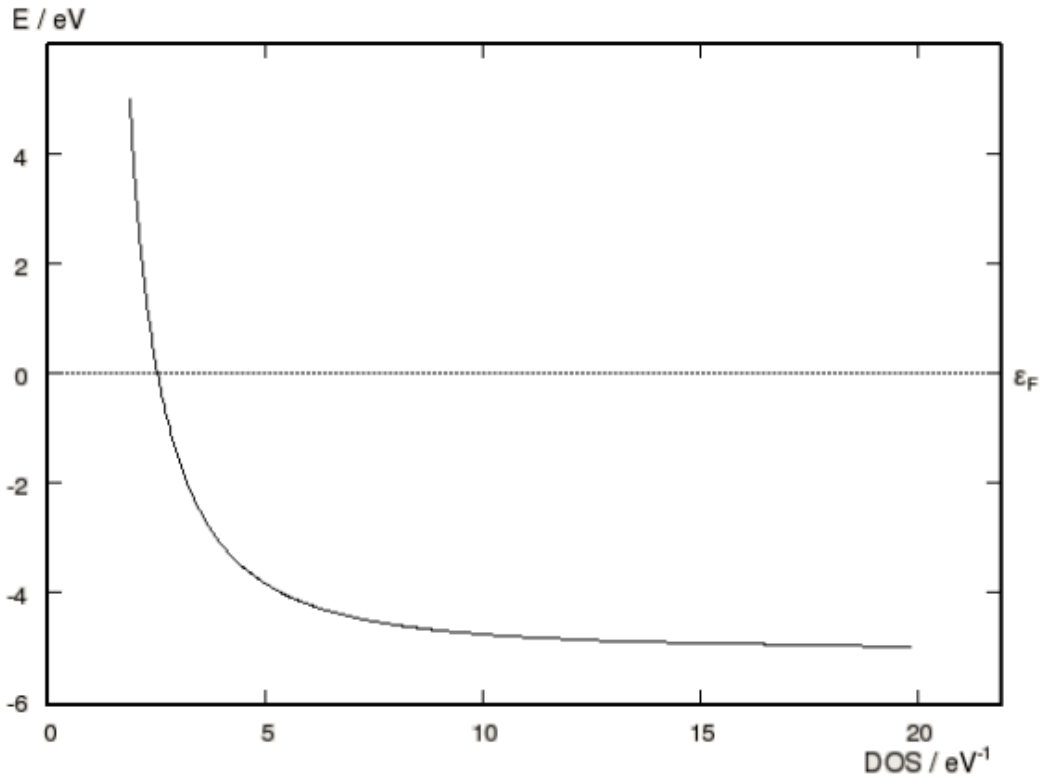

Figure 5.2: DOS of a pure C chain without spin

Figure 5.1 illustrates the transmission spectrum of C chain, a monatomic system. It is observed that transmittance, T(E), is constant at all energy values, as expected for a one dimensional pure system, Since both spin up and spin down channels contribute, the T(E) becomes 2. Figure 5.2 shows the variation of DOS of the same system. It gives the usual behavior expected for one dimensional system. We see that DOS is non zero at the Fermi level, which is zero eV. Therefore this system has a metallic property.

In spin polarization calculations, the magnitude of the polarization depends on SWN topology and atoms in the system. In Figures 5.3 and 5.4, spin dependent current (I) – bias (V) and conductance (G) – bias (V) characteristics, respectively, for C chain are shown. As shown in the figures, no spin polarization is observed (no spin asymmetry) for this monatomic system. Spin up (down) current linearly increases with bias applied between LL and RL. Spin dependent G is approximately constant with a trivial difference, especially between 0.6 - 0.8 V, where conductance becomes minimum for both spin states.

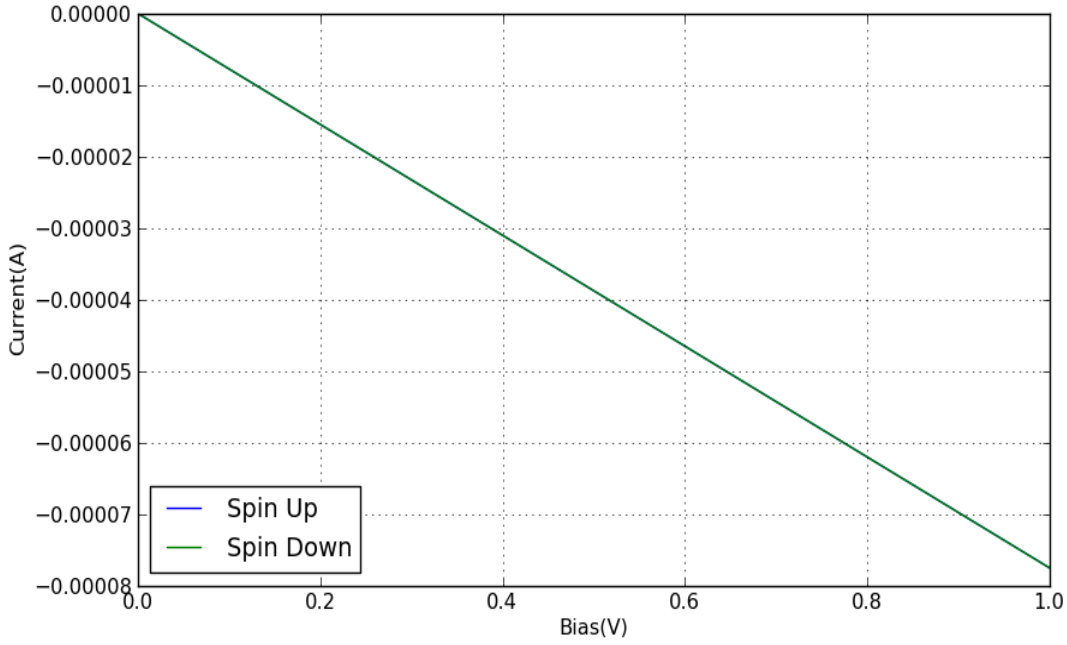

Figure 5.3: Spin dependent I – V curve of a pure C chain.

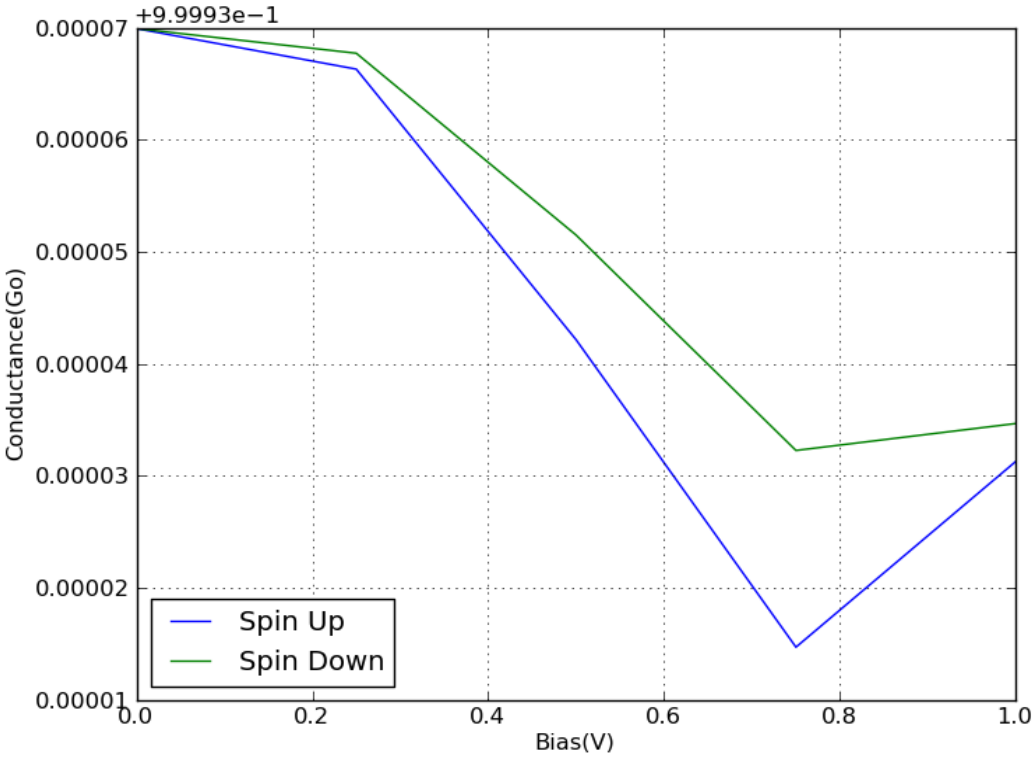

Figure 5.4: Spin dependent G – V plot of a C chain

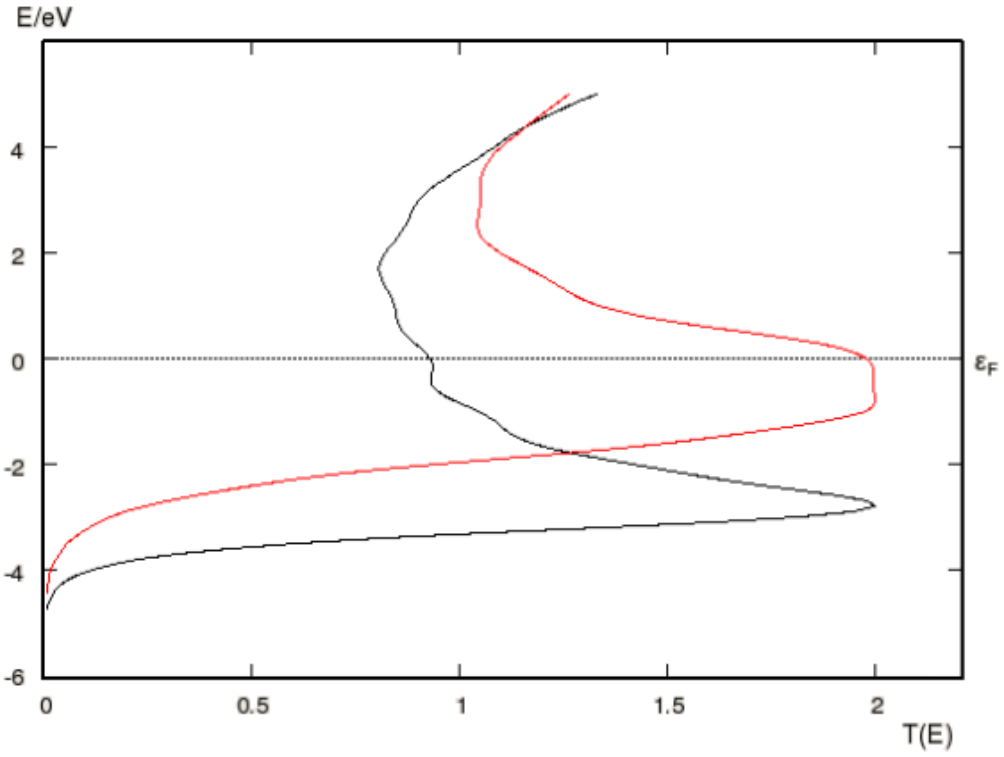

Figure 5.5: Spin dependent transmission spectrum of C chain with a Co impurity (Black curve: Spin up; Red curve: Spin down).

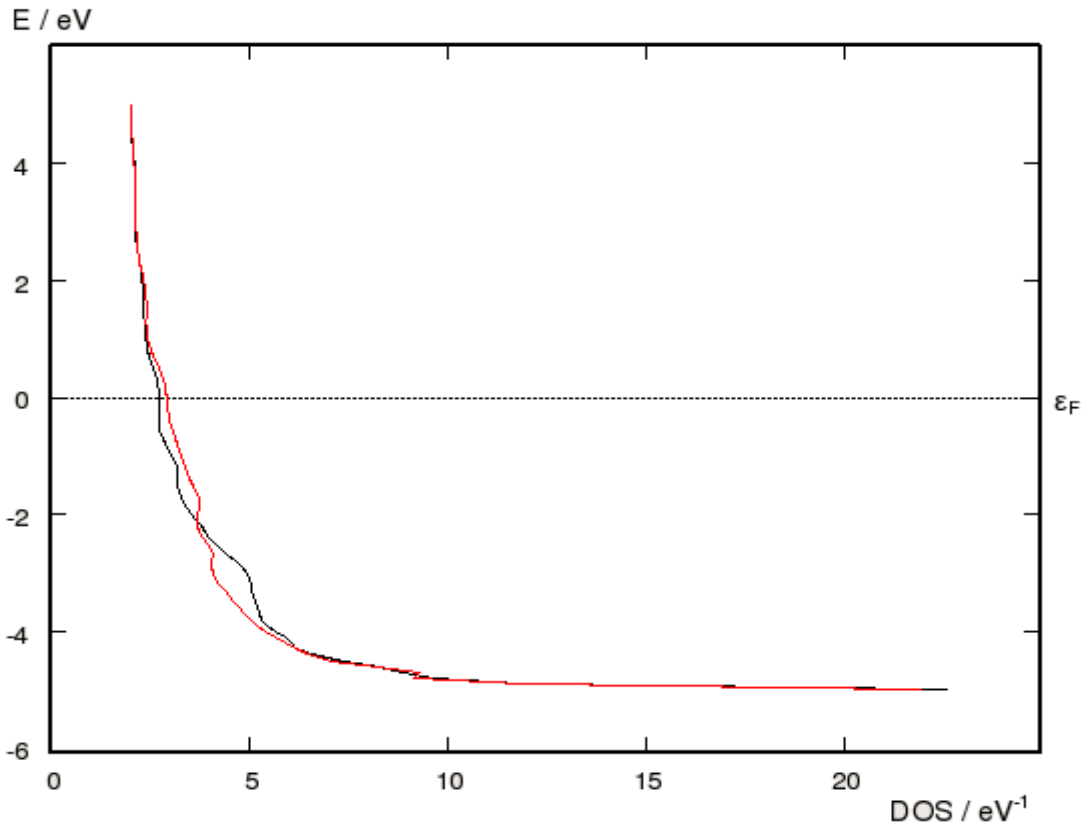

Figure 5.6: Spin dependent DOS of C chain with a Co impurity.

It is known that the characteristics of a monatomic C chain depends on number of atoms together with the type of impurities. As seen in Figure 5.5, adding a single Co impurity atom changes transmission significantly (Black curve: Spin up; Red curve: Spin down). It gives rise to maximum spin down transmittance at the Fermi energy. We see the spin polarization clearly. Figure 5.6 shows that the DOS becomes spin dependent especially around the Fermi level. Thus there is no symmetry between spin up and spin down curves, i.e. spin asymmetry as a result of Co impurity which is a transition element.

We have both focused on topological and substitutional disorder. In this way we are able to get information about their contributions on transport. For instance, Figures 5.7 – 5.10 give numerical results for C chain plus 2 bonds without impurities.

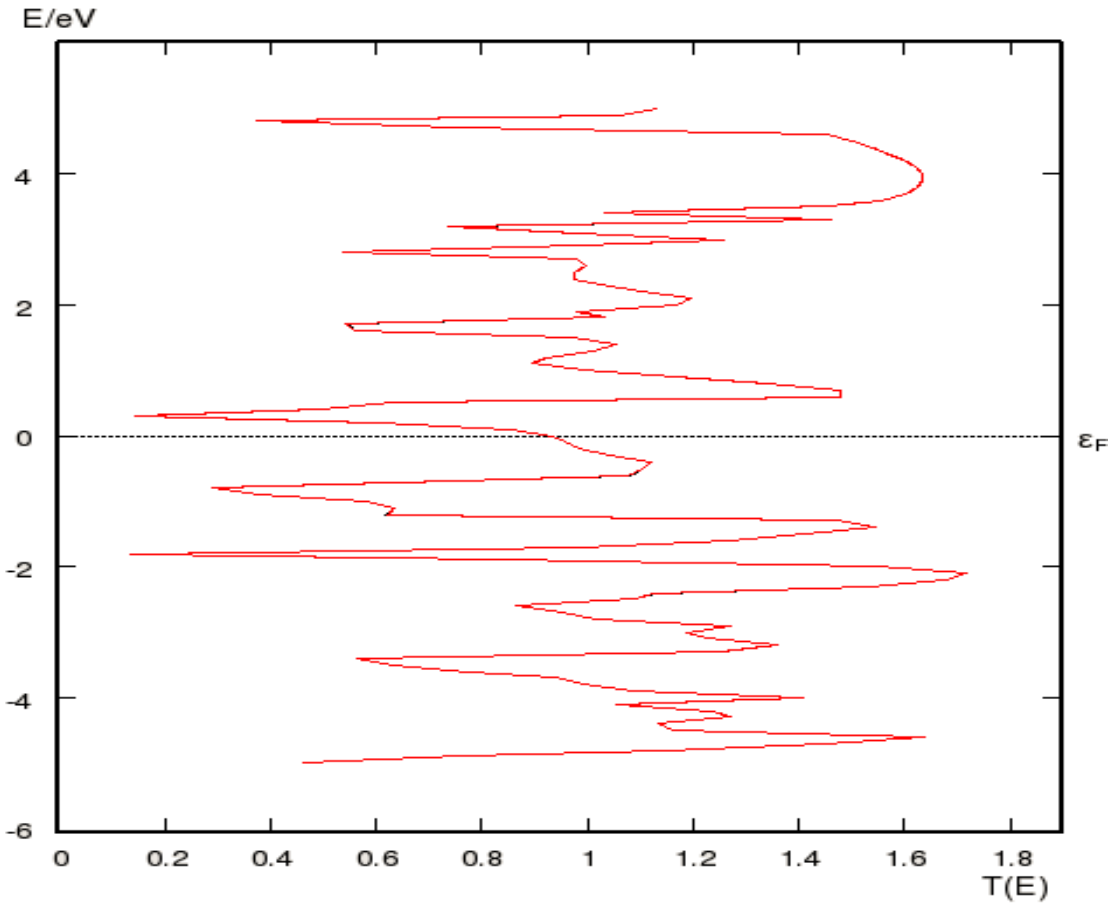

Figure 5.7: Transmission spectrum of C chain plus 2 bonds.

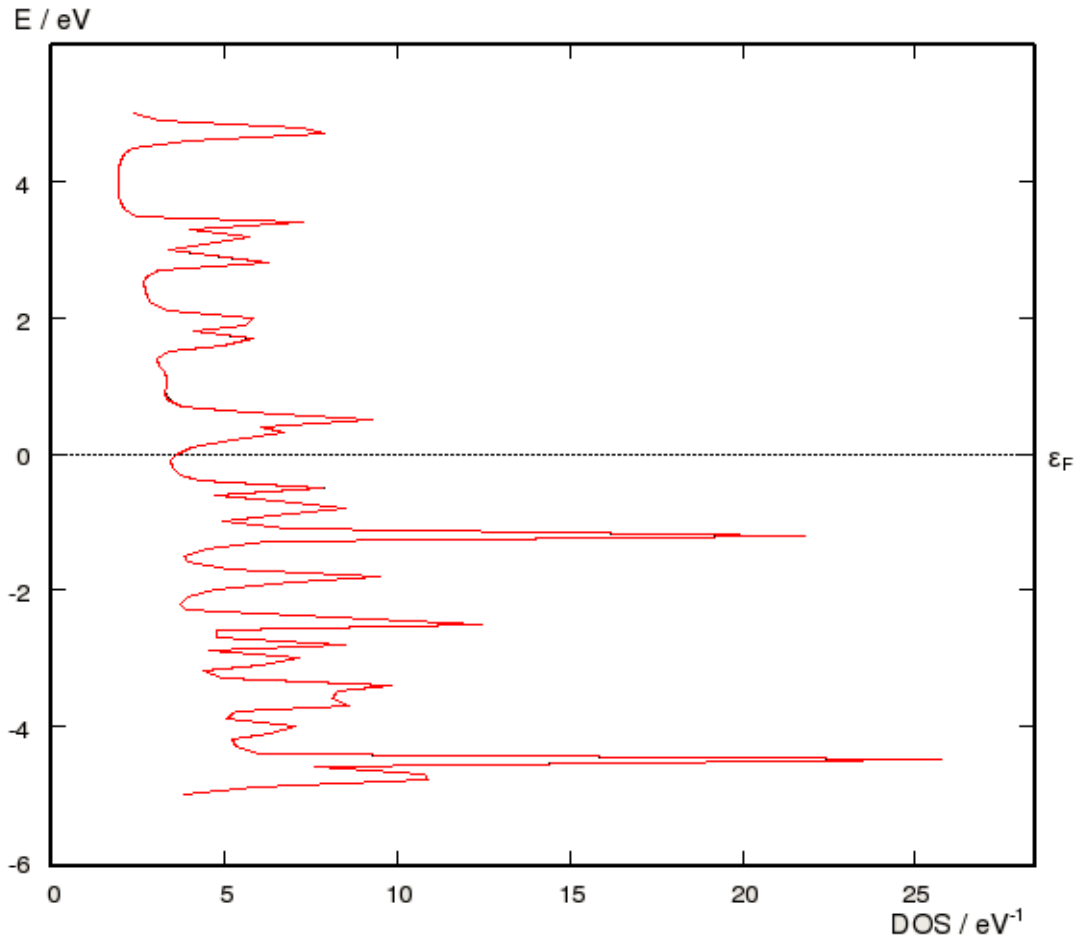

Figure 5.8: DOS of C chain plus 2 bonds.

As illustrated, in Figures 5.7 and 5.8, fluctuations in transmittance and DOS are observed, without getting spin dependence. These fluctuations arise from the disorder in geometry due to the scattering atoms on bonds. One deduce that without impurity, two bonds are not sufficient to get spin polarization. The system has a metallic property as DOS is finite at the Fermi level.

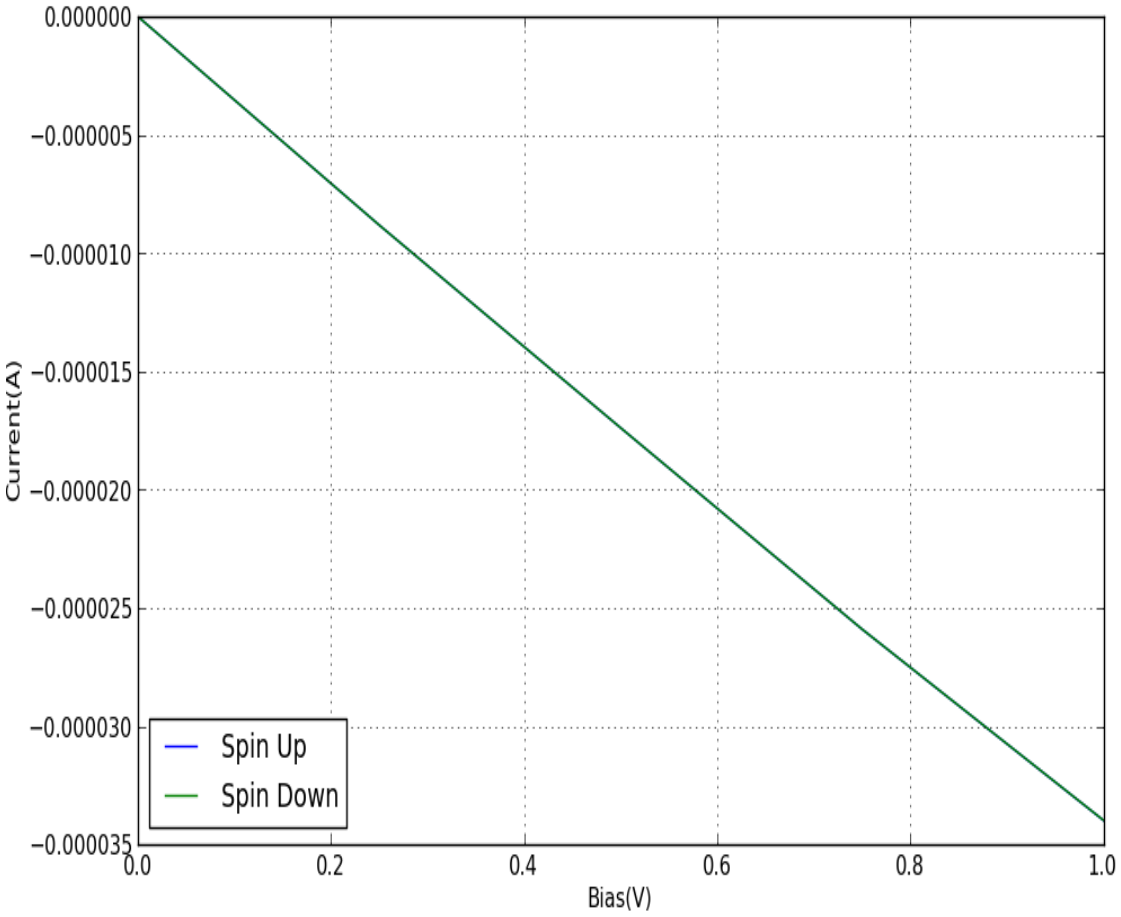

Figure 5.9: I – V graph of C chain plus 2 bonds.

For both spin states the current increases linearly as a function of bias voltage (Figure 5.9). Because of the geometrical disorder, here we get smaller current compared to C chain, at particular voltages. As shown in Figure 5.10, conductance becomes minimum at 0.75 Volt and starts to increase. This voltage is regarded as a critical voltage, which is related to low bias limit.

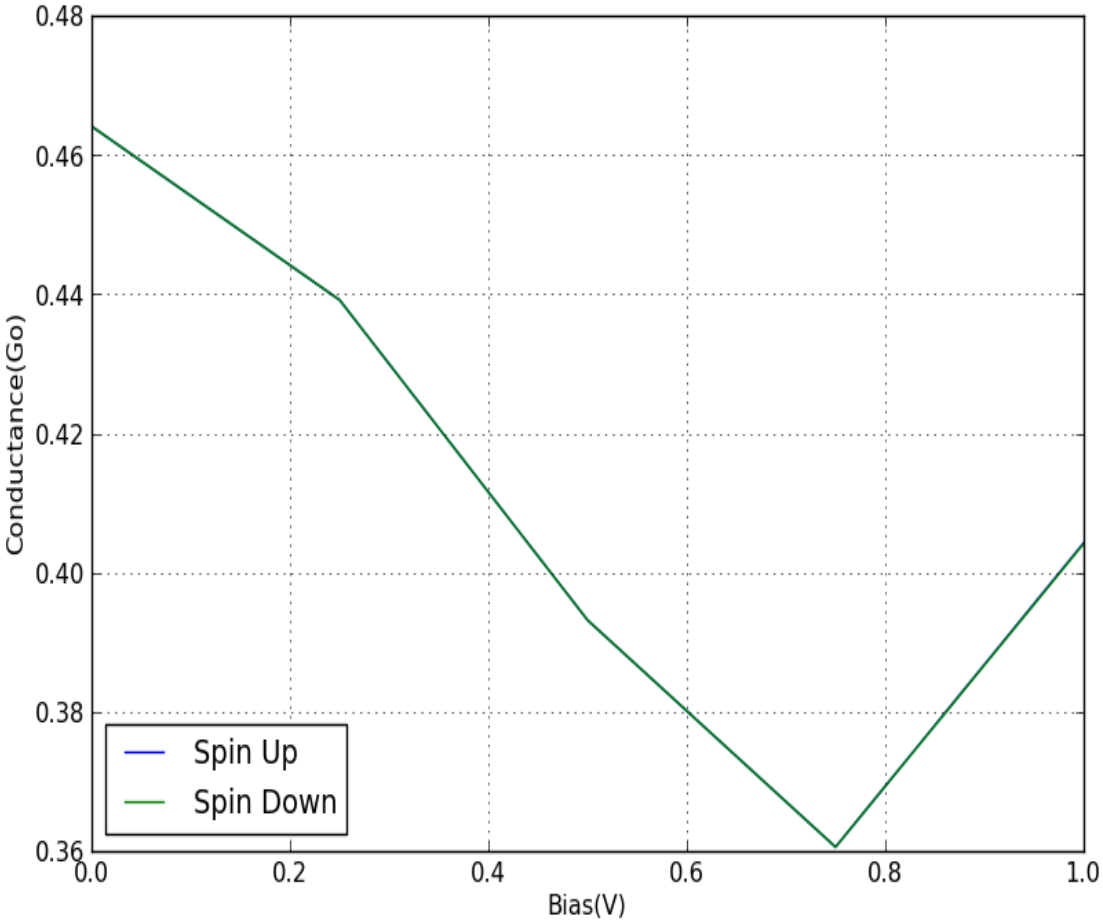

Figure 5.10: Conductance of C chain plus 2 bonds.

In order to have an idea about the effect of bonds, we increase the probability in SWN theory to obtain more bonds. When the system has four bonds we have observed spin polarization, even in the absence of impurities (see Figures 5.11 – 5.14). Notice that the increase number of fluctuations as a result of increase in bonds. There are peaks and dips in transmission spectra and no symmetry with respect to the Fermi level.

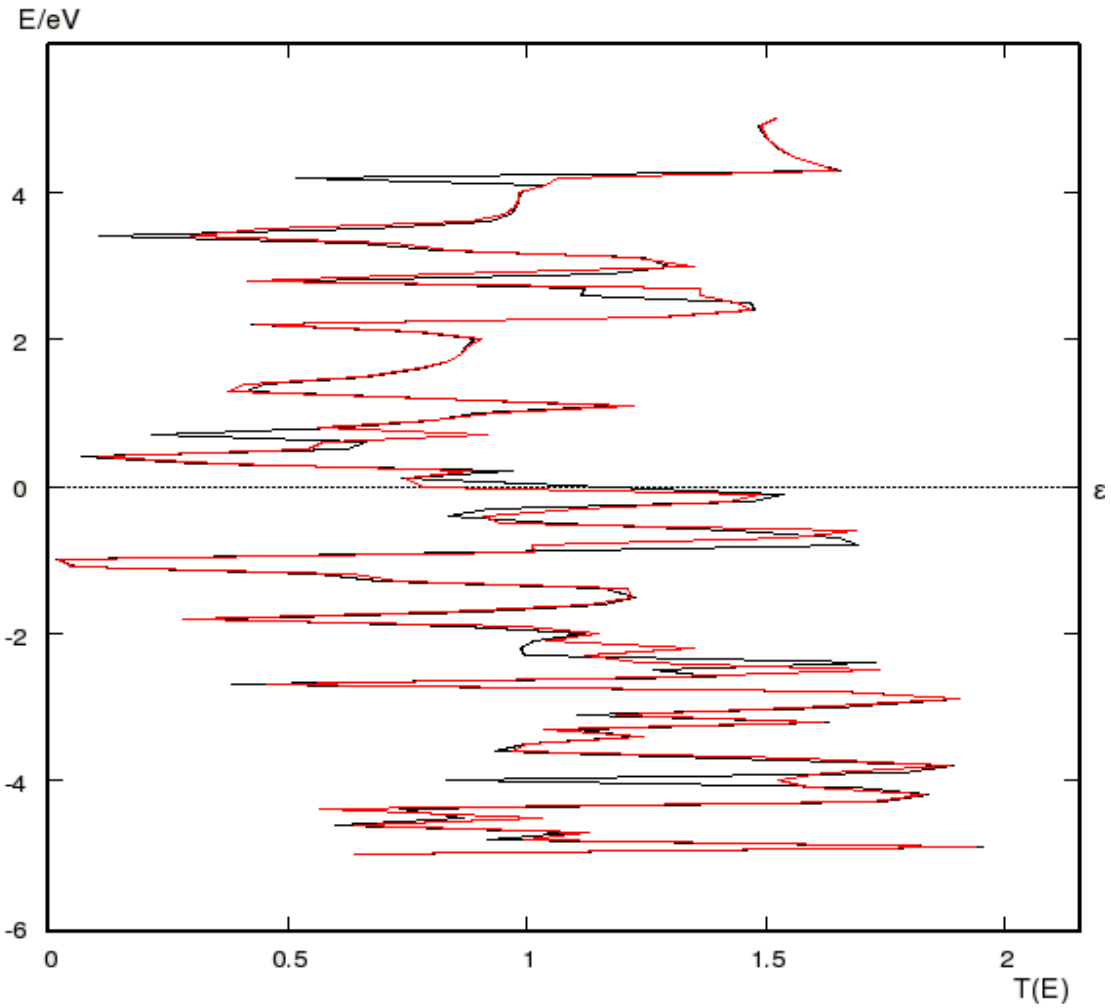

Figure 5.11: Transmission spectrum of C chain plus 4 bonds.

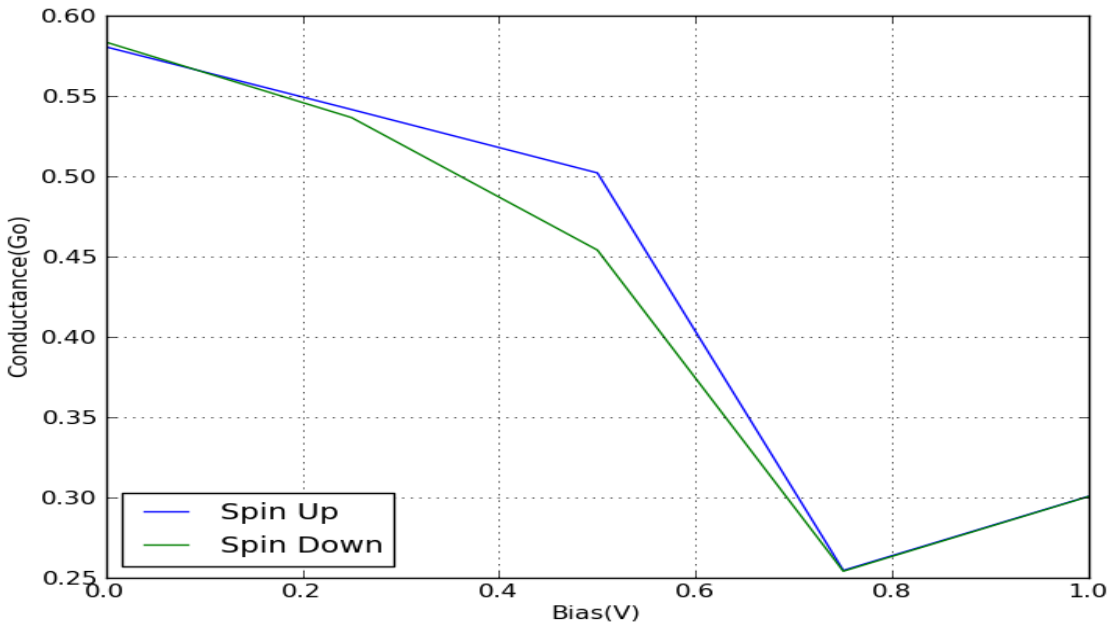

Figure 5.12: G – V graph of C chain plus 4 bonds.

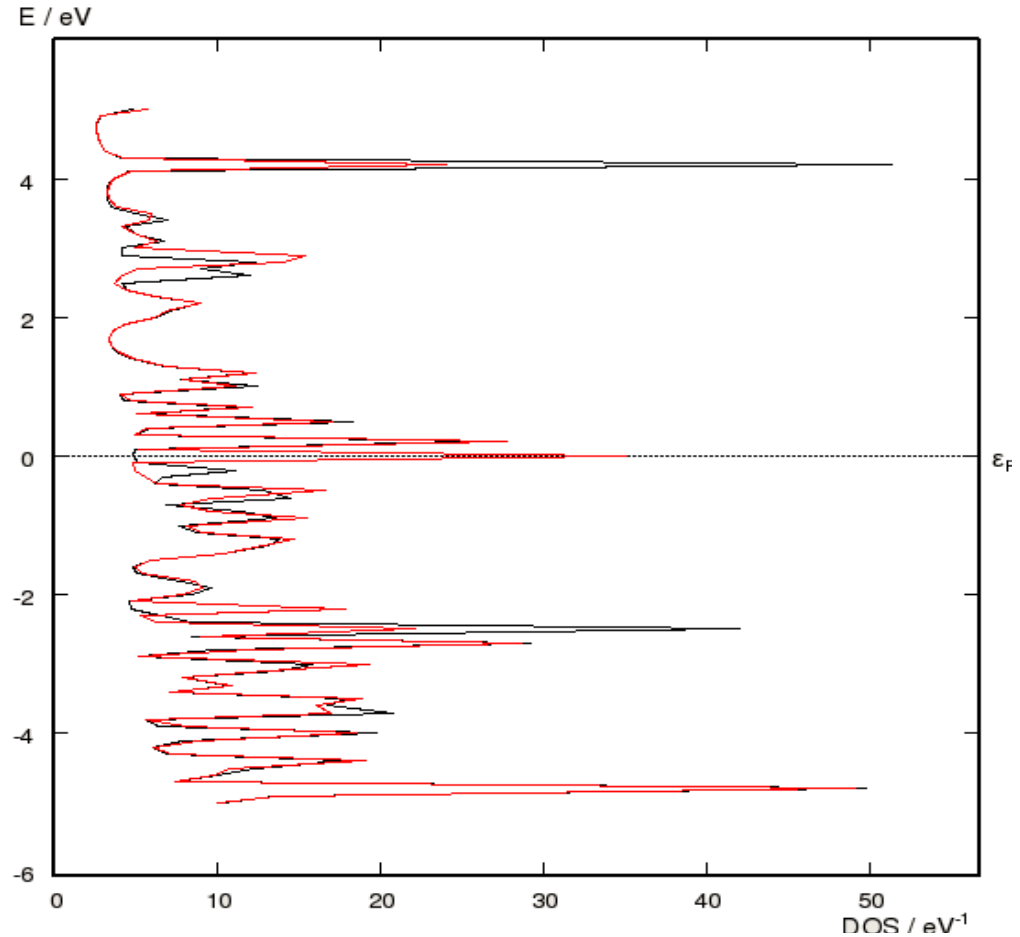

Figure 5.13: DOS of C chain plus 4 C bonds.

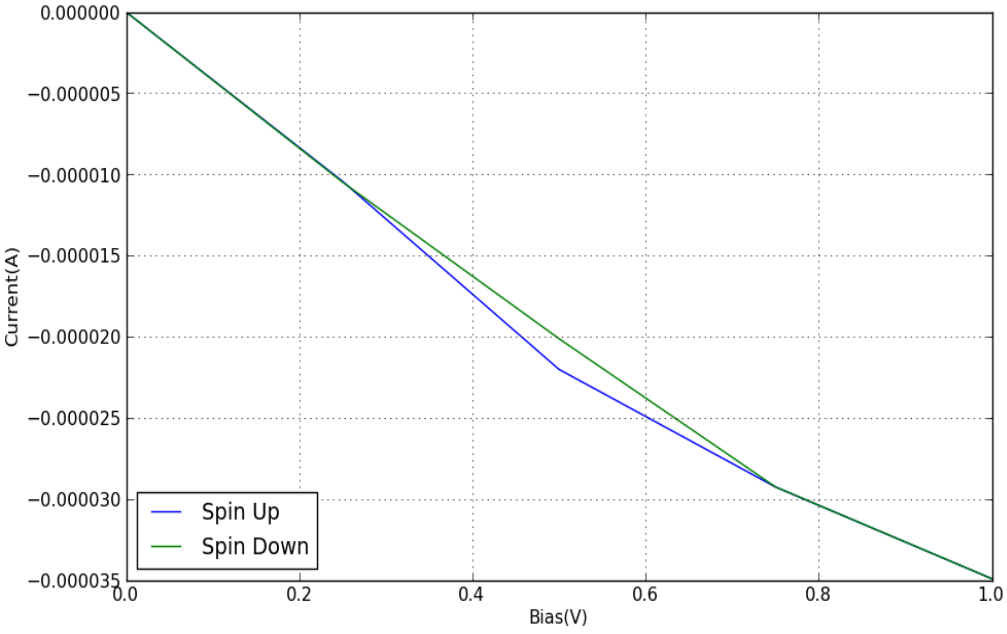

Figure 5.14: I - V plot of C chain plus 4 bonds.

Figure 5.12 illustrates the spin polarized conductance which becomes minimum again at the critical voltage, 0.75 Volt. The spin polarized DOS increases as a function of energy with fluctuations (Figure 5.13). It is seen that inserting the four bonds has a positive effect on conductance as it increases at specific biases. Increasing number of bonds affects the spin polarized current. After the critical voltage and up to 0.25 Volt spin polarization vanishes (Figure 5.14).

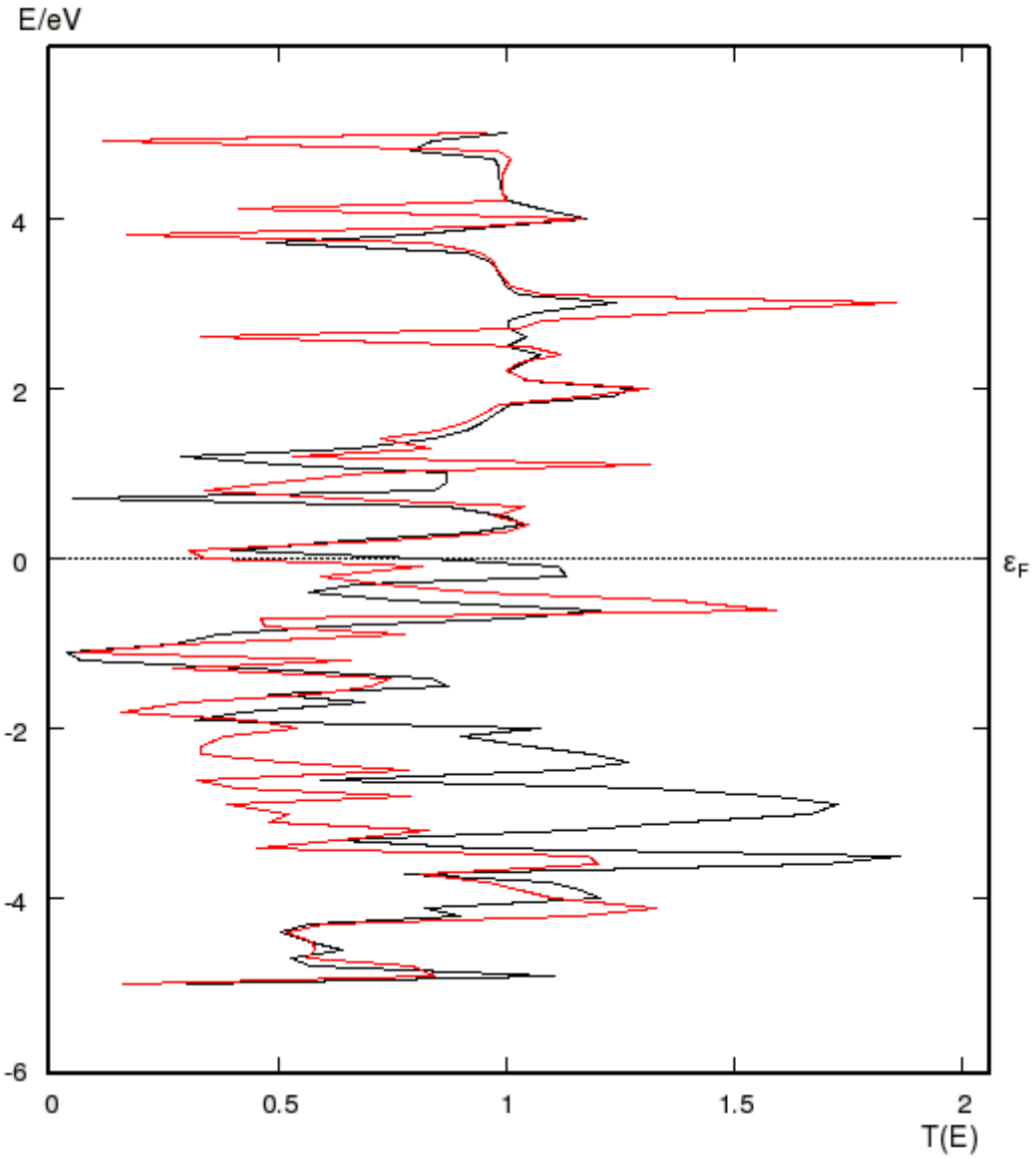

Figure 5.15: Transmission spectrum of C chain plus 4 bonds with Co impurities

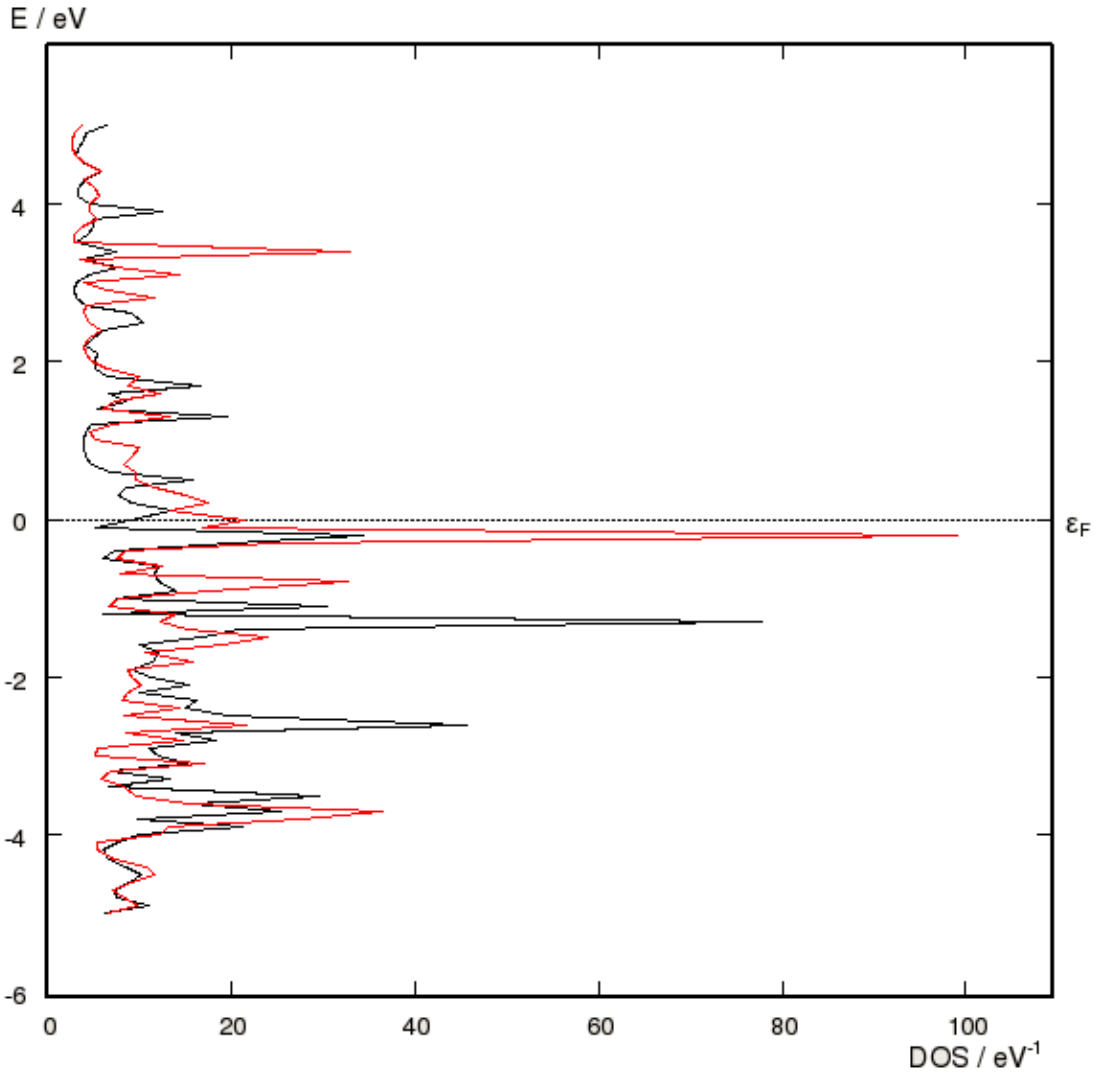

Figure 5.16: DOS of C chain plus 4 bonds with Co impurities.

We have also added Co impurities to SWN systems. Figures 5.15 – 5.18 represent the results for C chain plus four bonds with Co impurities on the main chain and bonds. Co atom has a crucial effect on spin polarization and so spin dependent transport. It is clearly observed that Co atom raises the spin polarization especially around the Fermi level (see Figure 5.15 and 5.16). It is a transition metal and in these metals *d* orbital plays the main role. For all low bias voltages (0.0 – 1.0 Volt) it is obvious that we get spin polarization (see Figure 5.17 and 5.18). Spin down DOS increases abruptly around the Fermi energy, giving rise to a certain appearance in spin polarization, as shown in Figure 5.16.

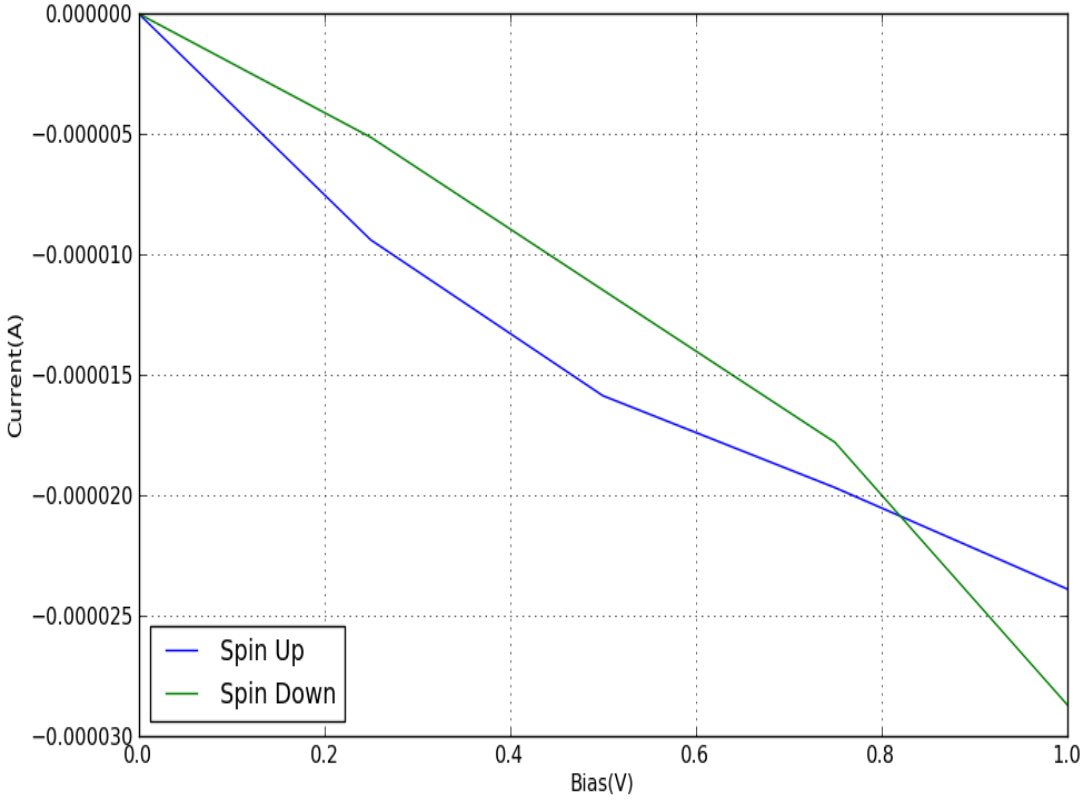

Figure 5.17: I – V plot of C chain plus 4 bonds with Co impurities.

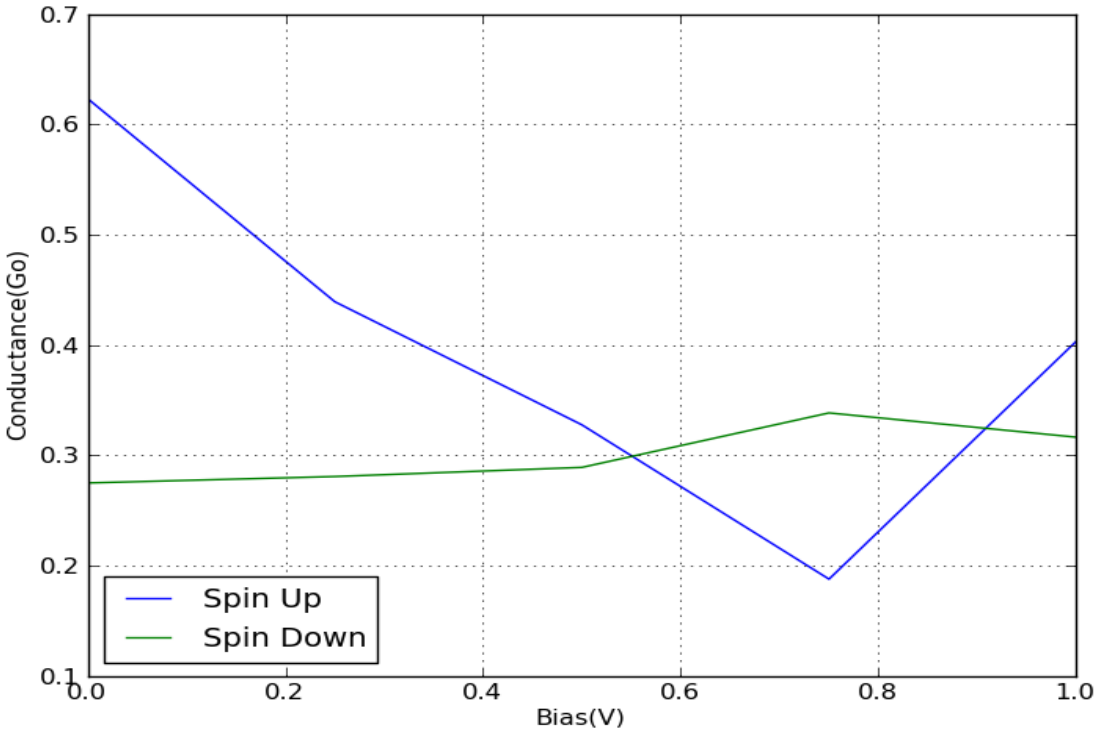

Figure 5.18: G – V plot of C chain plus 4 bonds with Co impurities.

In addition to Co atoms, we have considered H impurities as well. We have located H atoms by utilizing uniform distribution. Figures 5.19 and 5.21 show the spin dependent results for C chain plus four bonds with H impurities. It is known that transport is suppressed as a result of H atoms, yielding low transmittance around the Fermi level as observed in Figure 5.19. Here the emerging spin polarization is not due to H atoms but the number of bonds. We see the decrease in spin polarization in Figure 5.20, upon adding H atoms.

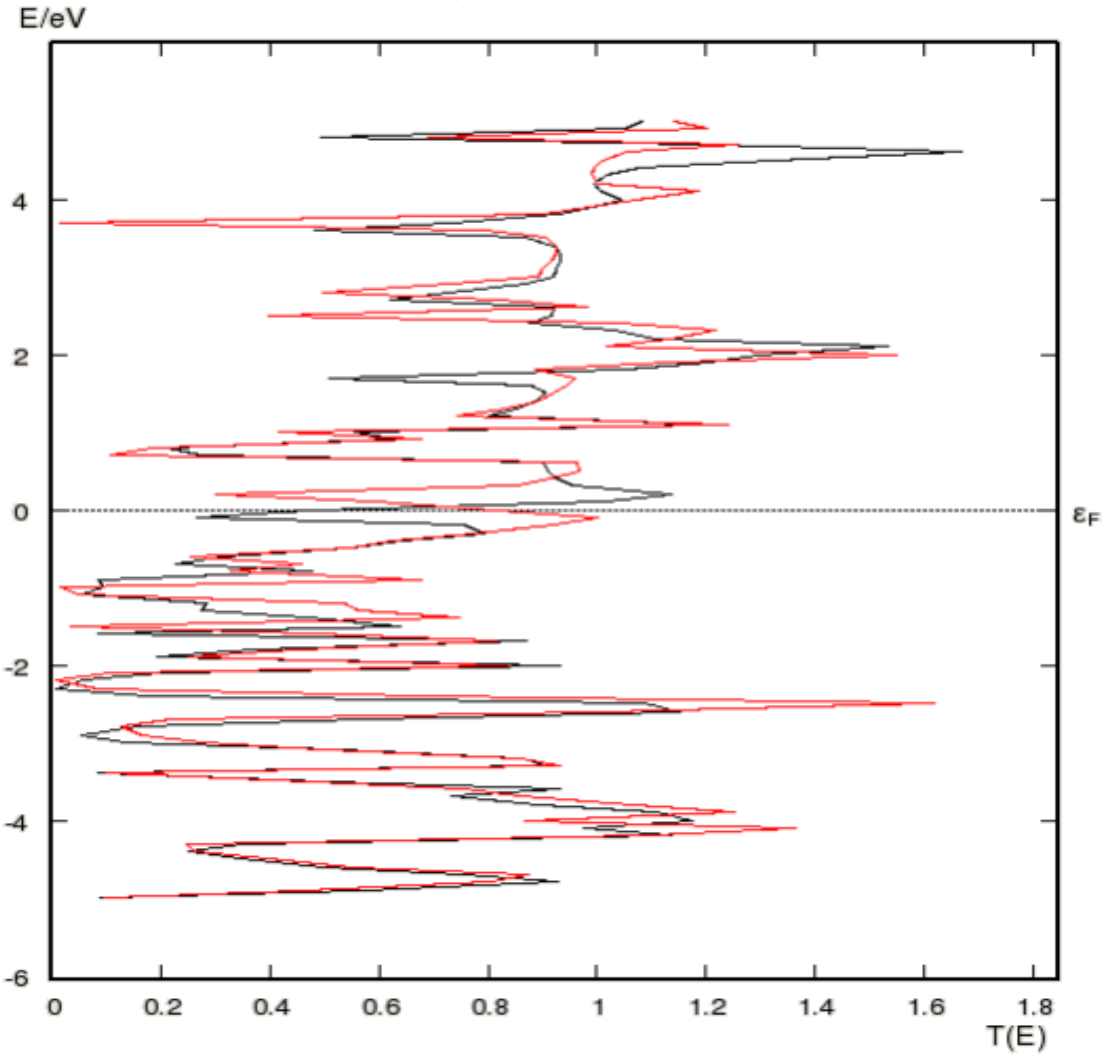

Figure 5.19: Transmission spectrum of C chain plus 4 bonds with H impurities.

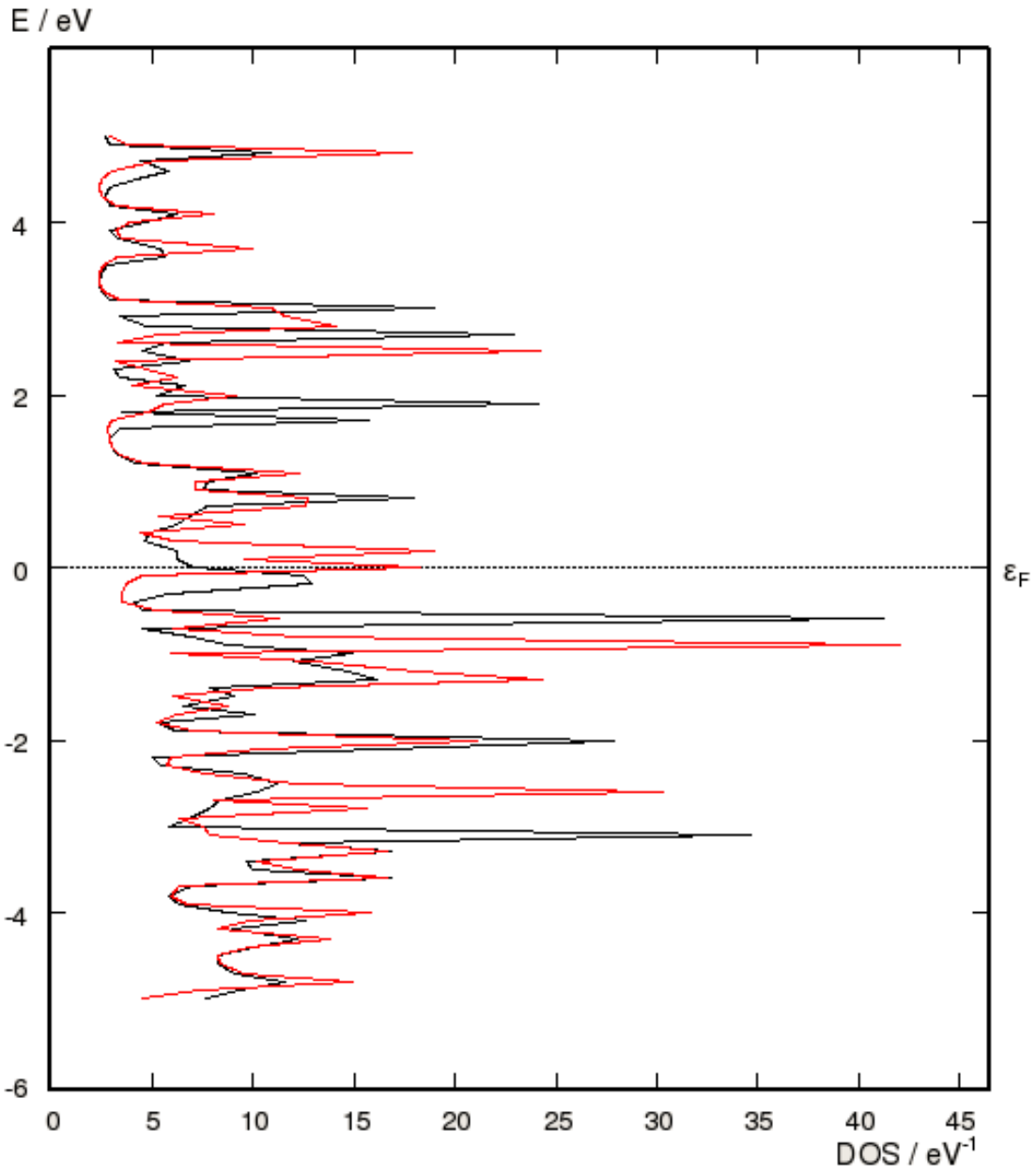

Figure 5.20: DOS of C chain plus 4 bonds with H impurities.

Spin polarized current is also significantly affected by H impurities (Figure 5.21). The linear increase in current is arising from short-cut paths defined in SWN theory. But spin polarization is suppressed.

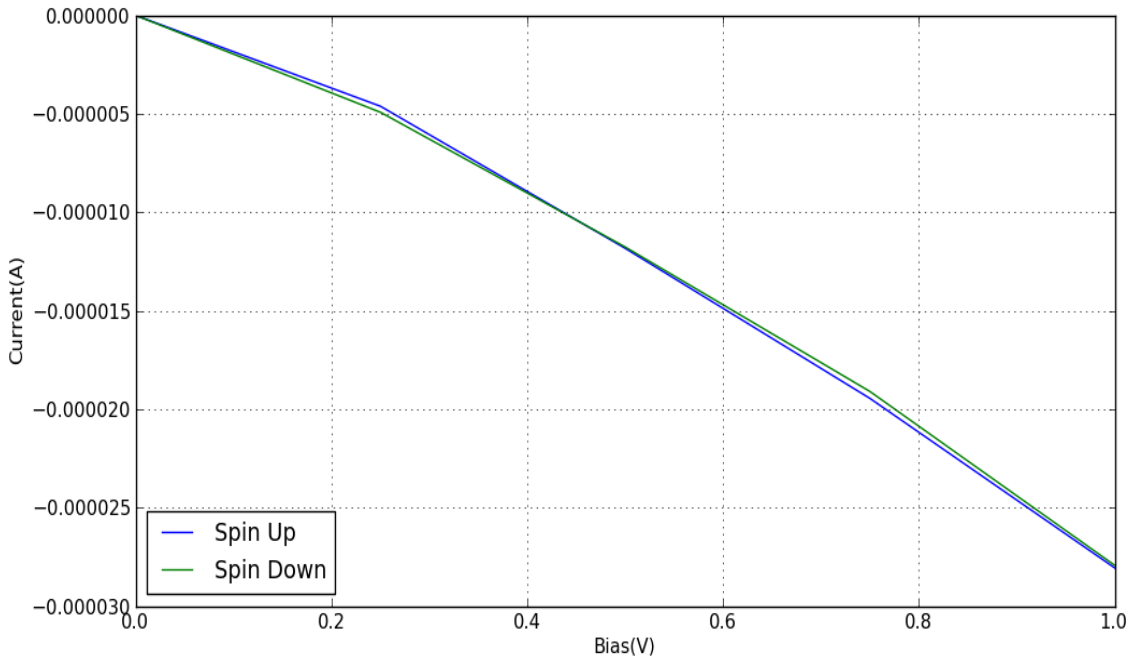

Figure 5.21: I –V curve of C chain plus 4 bonds with H impurities.

In order to demonstrate effect of electrodes, we have inserted Ni atoms on the LL and RL. Note that in the previous results, LL and RL contains monatomic C chains. Figure 5.22 to 5.27 give SWN systems between either parallel or antiparallel polarized Ni electrodes.

In Figure 5.22 and 5.23 we see the modification of transmittance when the SWN system consisting of C chain plus 6 bonds is placed between parallel and antiparallel polarized Ni electrodes, respectively. Even in the absence of Co atoms a well defined spin polarization is obtained at particular energies. This property related to magnetic Ni electrodes together with SWN topology, given by number and distribution of bonds. As seen in the figures, increasing number of bonds provide more fluctuations in the transmission.

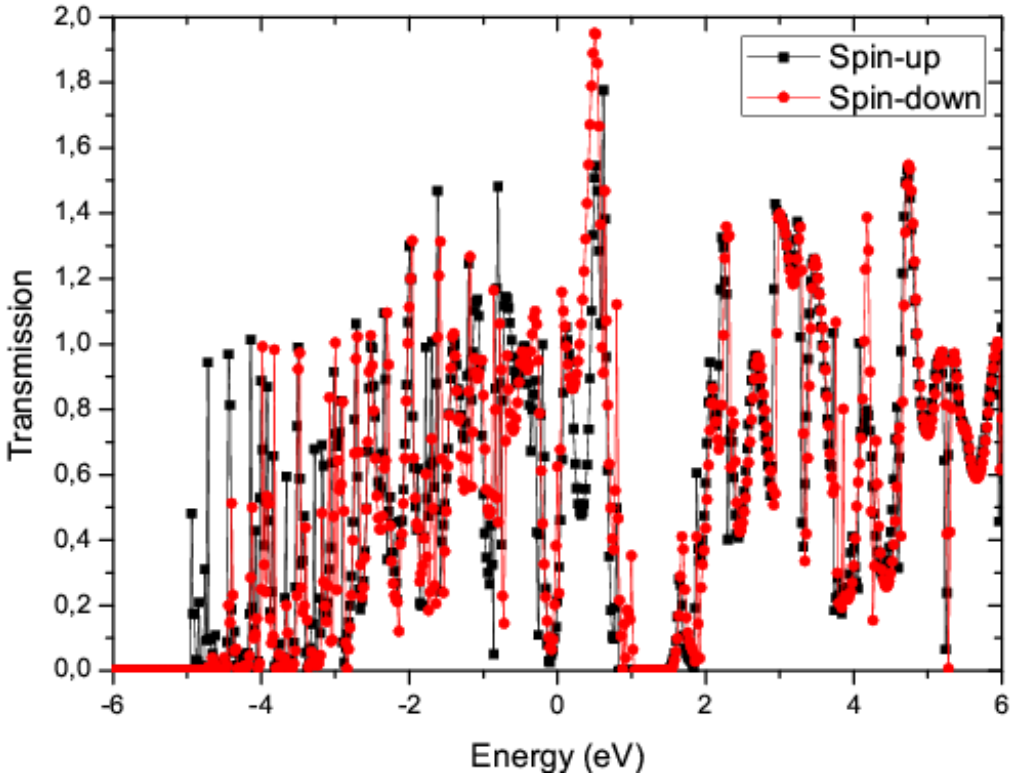

Figure 5.22: Transmission of C chain plus 6 bonds between parallel Ni electrodes.

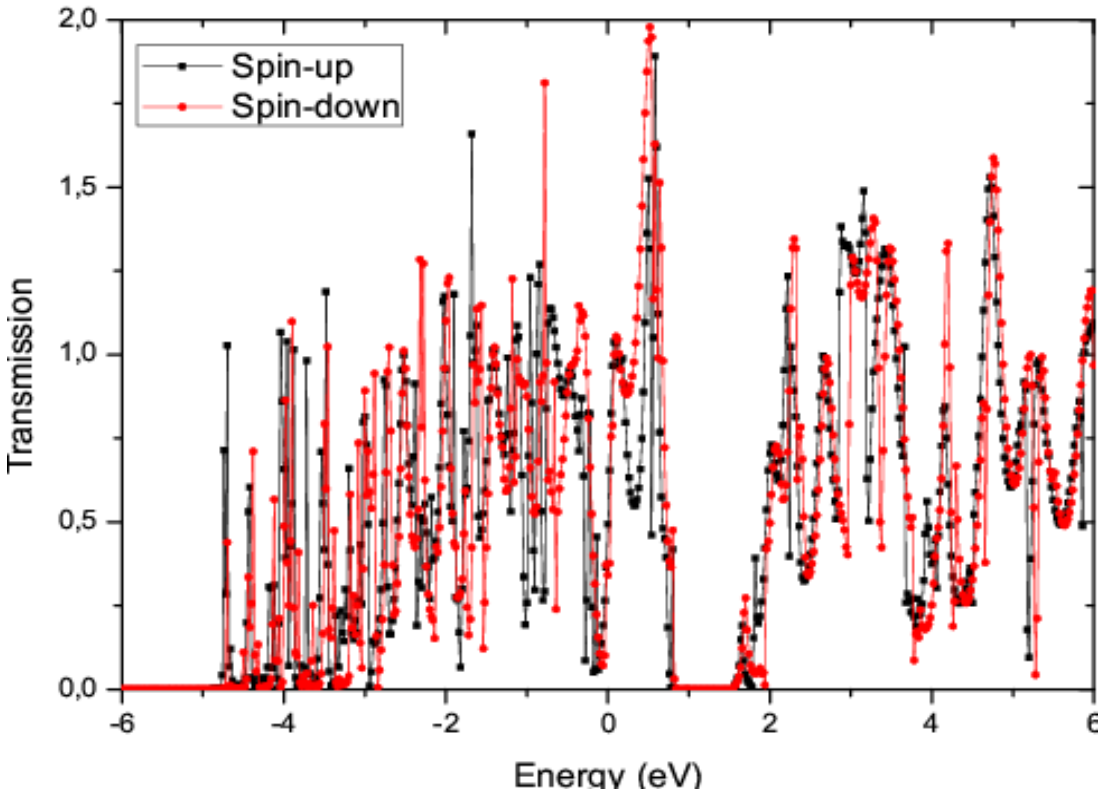

Figure 5.23: Transmission of C chain plus 6 bonds between antiparallel Ni electrodes

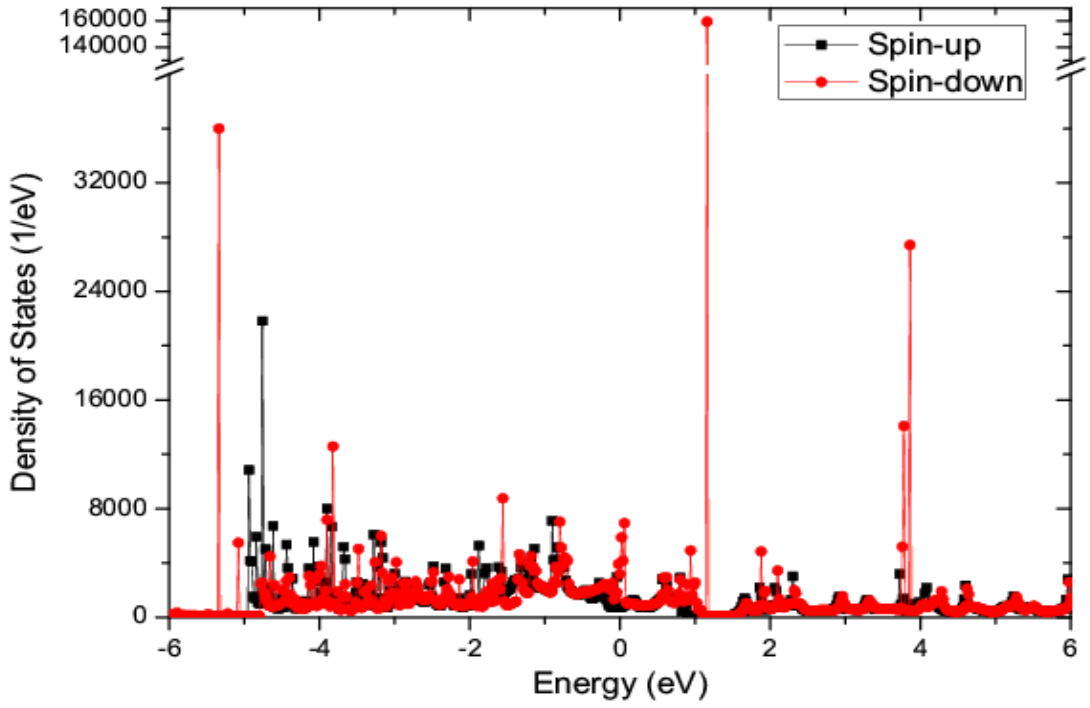

Figure 5.24: DOS of C chain plus 6 bonds between parallel Ni electrodes.

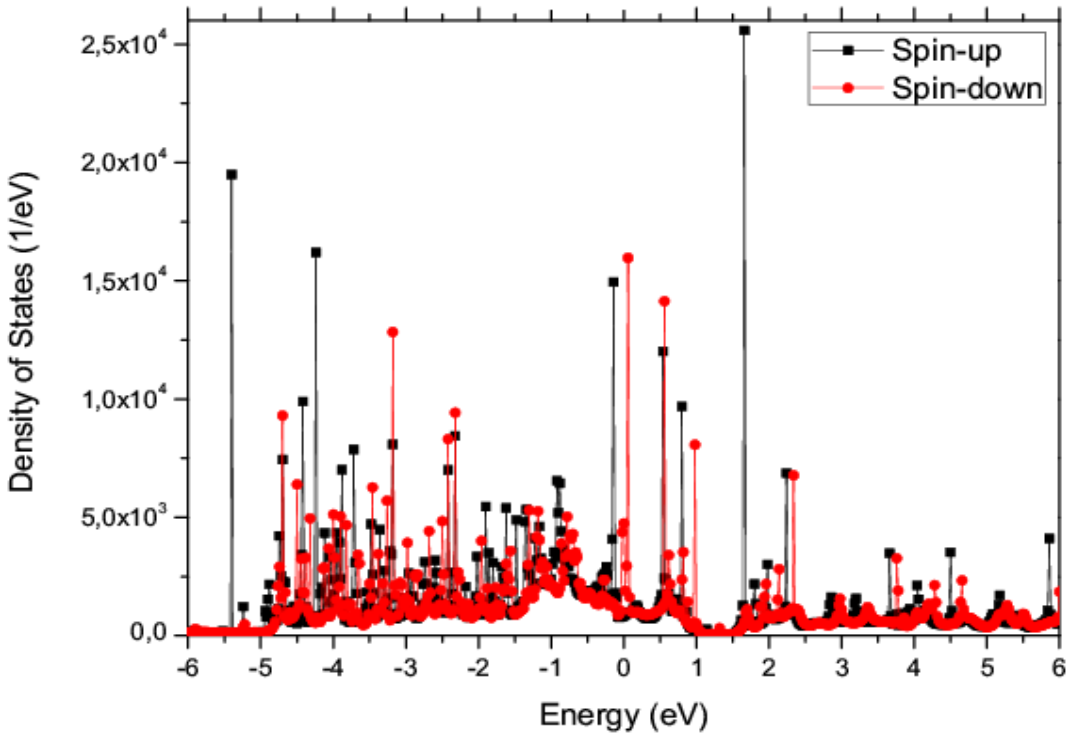

Figure 5.25: DOS of C chain plus 6 bonds between antiparallel Ni electrodes.

Figure 5.24 and 5.25 give the behavior of DOS having many fluctuations in both spin orientations. Parallel Ni electrodes enormous spin down DOS peaks at the energies given in the figures. Antiparallel ones approximately give an equal number of spin up and down peaks at specific energies. The resonances are due to the fact that eigenvalues coincide with energy of electrons.

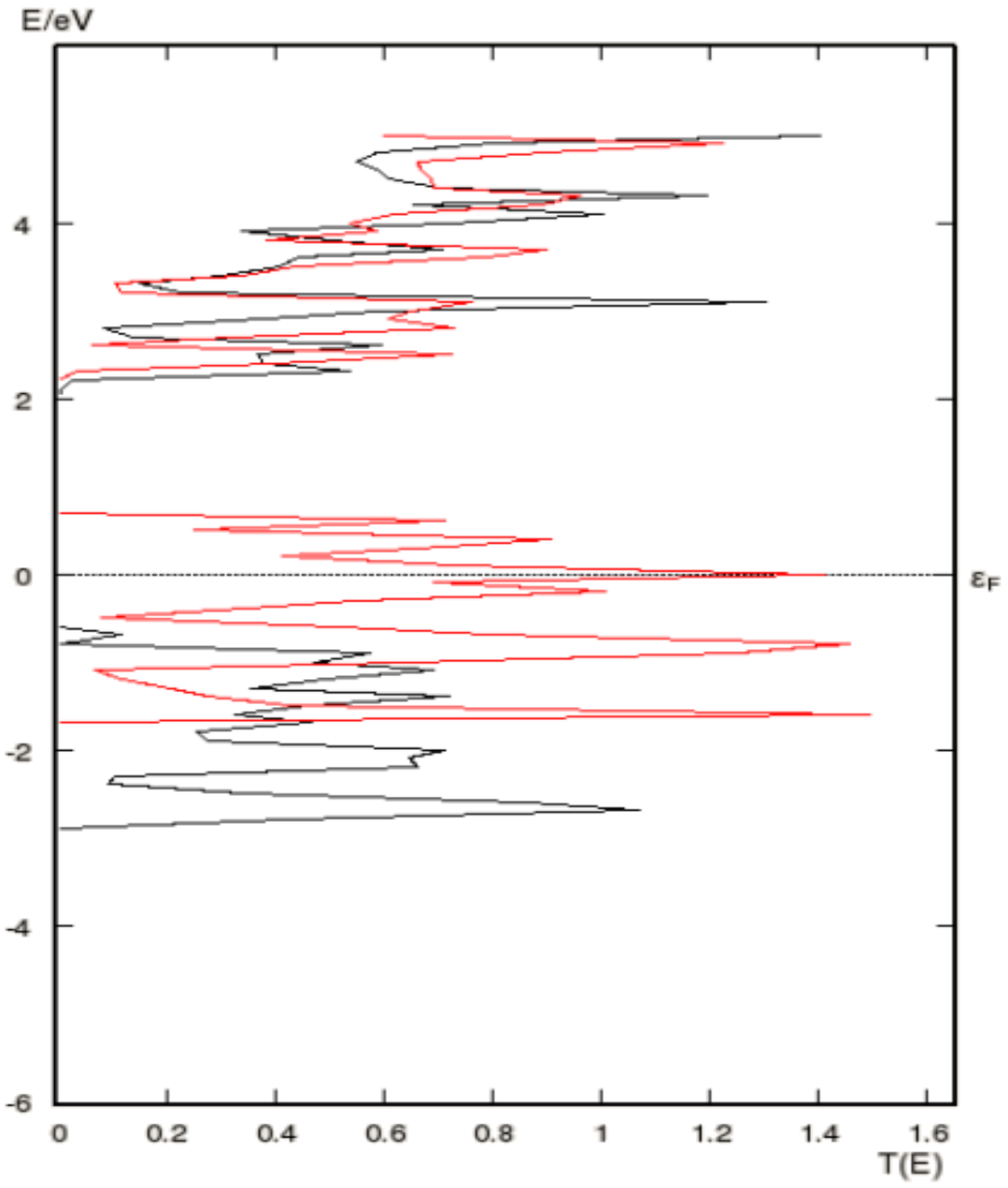

Figure 5.26: Transmission of C chain plus 4 bonds with Co impurities between parallel Ni electrodes.

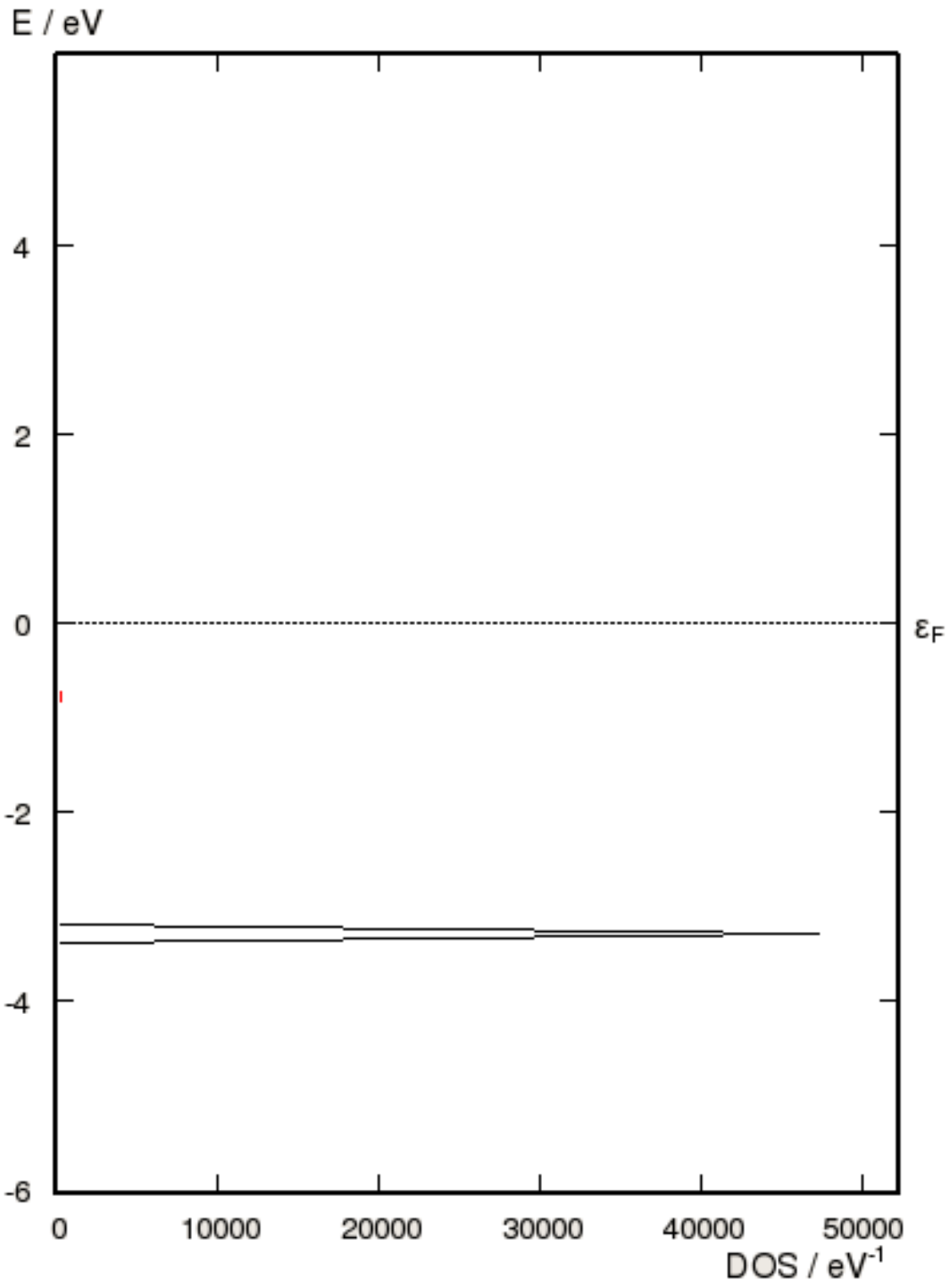

Figure 5.27: DOS of C chain plus 4 bonds with Co impurities between parallel Ni electrodes.

In Figures 5.26 and 5.27, we have results for SWN systems containing Co impurities between parallel Ni electrodes. The combined effect arising from polarized Ni electrodes and spin introduced Co atoms in the system is clearly seen. Figure 5.26

gives the behavior of transmittance and Figure 5.27 presents that of DOS. In these figures we observe that at some energy ranges only one spin state contributes, yielding a perfect spin polarization. The DOS is zero in the energy range including the Fermi level, meaning that the corresponding system has not metallic property.

CHAPTER 6

CONCLUSIONS

Small World Networks, including Co atoms as well, are established on Carbon based linear atomic chain. In calculations, we have employed ATK software package, which is based on DFT combined with NEGF method. We have found minima in the transmission spectra. These minima have been analyzed through transmission eigenchannel analysis, yielding that dips in the transmission are due to depressions of eigenchannels for each spin. One of the reasons may be weak coupling between electrodes and central system, a general outcome. There are also discontinuities in some spectra, which may arise due to coupling between localized states in SWN and continuous states of electrodes.

One of the most important results we have found is that spin polarized electronic band structures and transport depend crucially on the property of configuration of the network (geometry of the system, i.e the distribution of bonds and length of them). The electronic transport is also influenced by the chosen electrodes as the transport depends on the atomic structure of them.

Even in the absence of transition elements taken as substitutional impurities we have obtained spin polarization. It is due to the fact that spin polarization and so spin asymmetry may also arise due to interaction between electrodes and system (due to special or partial contact) and SWN geometry. It is known that the type of the impurity, for instance, whether a transition atom or not, and localization length are critical in getting the spin polarized transport. Co is a transition atom and gives rise to spin polarization: Exchange interaction between the Co atoms through the C atoms on the main chain and bonds result in induced magnetic moments on C atoms and spinpolarization, because of asymmetric coupling between Co and C. For the systems, consisting of C chain with SW bonds plus Co, we have considered it is seen

that polarization is preserved and spin coherence can easily be maintained. It leads interesting spin dependent properties needed for constructing spintronics devices.

If the number of bonds in SWN is sufficiently high (i.e, close to max probability), one may expect instabilities and localization of impurities. These are related to the topology of the SWN and yield the spin dependent transport property of the systems. Thus the behaviors of spin dependent transport quantities are fingerprints for the SWN topology.

REFERENCES

[1] R. G. Parr, W. Yang, Oxford University Press, New York, 1989.

[2] P. Hohenberg, W. Kohn, *Phys. Rev.* Vol. 136, pp. 864, 1964.

[3] W. Kohn, L. J. Sham, *Phys. Rev. A.* Vol. 140, pp. 1133–1138, 1965.

[4] http://www.physik.unizh.ch/~sam/diss/node10.html.

[5] R. O. Jones, O. Gunnarsson, *Rev. Mod. Phys*. Vol. 61, pp. 689, 1989.

[6] John P. Perdew, J. A. Chevary and S. H. Vosko, Koblar A. Jackson, Mark. R. Perderson and D. J. Singh, Carlos Fiolhais, *Phys. Rev. B.* Vol. 46, pp. 6671–6687, 1992.

[7] A. D. Becke, *J. Chem. Phys.* Vol. 109, pp. 2092, 1998.

[8] J. P. Perdew, S. Kurth, A. Zupan and P. Blaha, *Phys. Rev. Lett*. Vol. 82, pp. 2544, 1999.

[9] Ferdows Zahid, Magnus Paulsson and Supriyo Datta, Academic Press, pp. 17-22, 2003.

[10] S. Sanvito, *Handbook of Computational Nanotechnology*, pp. 54-56, 2005.

[11] R. Landauer, *IBM J. Res. Dev.* Vol. 1, pp. 223, 1957.

[12] R. Landauer, *Philos. Mag*. Vol 21, pp. 863, 1970.

[13] D. K. Ferry and S. M. Goodnick, Cambridge University Press, Cambridge, 1997.

[14] Supriyo Datta, Cambridge University Press, pp. 1-22, Cambridge, 1995.

[15] J. Fabian, A. Matos-Abiague, C. Ertler, P. Stano, I. Zutic, *Acta Physica Slovaca*, Vol. 57, pp. 565-907, 2007.

[16] Igor Zutic, Jaroslav Fabian, S. Das Sarma, *Rev. Mod. Phys*, Vol. 76, pp. 323-410, 2004.

[17] S. A. Crooker, D. L. Smith, *LALP*-05-143, 2006.

[18] Jaroslav Fabian, Alex Matos-Abiague, Christian Ertler, Peter Stano, Igor Zutic, *Acta Phys. Slovaca*, Vol. 57, 4–5, pp. 565–907, 2007.

[19] Albert Fert, *Nobel Lecture*, pp. 59-80, 2007.

[20] M. N. Baibich, J. M. Broto, A. Fert, F. Nguyen Van Dau, F. Petroff, P. Etienne, G. Creuzet, A. Friederich, and J. Chazelas, *Phys. Rev. Lett*. Vol. 61, pp. 2472, 1988.

[21] G. Binash, P. Grünberg, F. Saurenbach, and W. Zinn, *Phys. Rev. B.* Vol. 39, pp. 4828, 1989.

[22] J. Mathon and A. Umerski, *Phys. Rev. B.* Vol. 63, pp. 220403, 2001.

[23] J. S. Moodera, *Phys. Rev. Lett*. Vol. 74, pp. 3273–3276, 1995.

[24] S. Datta, B. Das, *Appl. Phys. Lett*. Vol. 56, pp. 665, 1990.

[25] S. Sugahara, M. Tanaka, *Appl. Phys. Lett*. Vol. 84, pp. 2307, 2004.

[26] S. Sugahara, M. Tanaka, *J. Appl. Phys.* Vol. 97, pp. 10D503, 2005.

[27] P. S. Anil Kumar and J. C. Lodder, *J. Phys. D: Appl. Phys.* Vol. 3, pp. 2911, 2000.

[28] E. I. Rashba, *Fiz. Tverd. Tela (*Leningrad) 2, pp. 1224, 1960, *Sov. Phys. Solid State* 2, pp. 1109, 1960.

[29] M. Johnson, *Science*, Vol. 260, pp. 320, 1993.

[30] N. Lebedeva, P. Kuivalainen, *J. Appl. Phys*. Vol. 93, pp. 9845, 2003.

[31] D. J. Watts, S. H. Strogatz, *Nature*, Vol. 393, pp. 409–410, 1998.

[32] Zengwang Xu, Daniel Z. Sui, *Journal of Geographical Systems*, Vol. 9, No. 2, pp. 189-205, 2007.

[33] S. Tongay, R.T. Senger, S. Dag, S. Ciraci, *Phys. Rev. Lett.* Vol. 93, pp. 136404, 2004.

[34] H. Ohnishi, Y. Kondo, K. Takayanagi, *Nature*, Vol. 395, pp. 780, 1998.

[35] Xinluo Zhao, Yoshinori Ando, Yi Liu, Makoto Jinno, and Tomoko Suzuki, *Phys. Rev. Lett.* Vol. 90, pp. 187401, 2003.

[36] H. Ding, J. P. Maier, *J. Phys. Conf. Ser. Vol.* 61, 2007.

[37] S. Sahoo, T. Kontos, J. Furer, C. Hoffmann, M. Gräber, A. Cottet, and C. Schönenberger, *Nature Phys.* Vol 1, pp. 99, 2005.

[38] N. Tombros, S. J. van der Molen, B. J. van Wees, *Phys. Rev. B.* Vol. 73, pp. 233403, 2006.

[39] Z. Y. Li, W. Sheng, Z. Y. Ning, Z. H. Zhang, Z. Q. Yang and H. Guo, *Phys. Rev. B*. Vol. 80, pp. 115429, 2009.

[40] S. Iijima, *Nature*, Vol. 354, pp. 56-58, 1991.

[41] H. Pan, T.H. Lin, D. Yu, *Eur. Phys. J. B*. Vol. 47, pp. 437–441, 2005.

[42] X. Q. Shi, Z. X. Dai, G. H. Zhong, X. H. Zheng, Z. Zeng, *J. Chem. Phys.* Vol. 111, pp. 10130-10134, 2007.

[43] K. Tsukagoshi, B.W. Alphenaar, H. Ago, *Nature*, Vol. 401, pp 572, 1999.

[44] B. Zhao, I. Monch, H. Vinzelberg, T. Muhl, C.M. Schneider, *Appl. Phys. Lett*. Vol. 80, pp. 3144, 2002.

[45] http://www.quantumwise.com

[46] M. Brandbyge, J. L. Mozos, P. Ordejón, J. Taylor and K. Stokbro. *Phys. Rev. B.* Vol. 65, pp. 165401, 2002.